Nucleon axial charge and the lowest moments of dimension-four operators from lattice QCD

Konstantin Ottnad

Nucleon Spin Structure at Low Q: A Hyperfine View

ECT* Trento, July 4th, 2018

JOHANNES GUTENBERG UNIVERSITÄT MAINZ

JG|U

SFB 1044 THE LOW-ENERGY FRONTIER OF THE STANDARD MODEL

HIM Helmholtz-Institut Mainz

PRISMA

Outline

1. Introduction
   - Operators, matrix elements, form factor decompositions
2. Lattice Setup
   - Ensembles
   - Computational details, renormalization ...
3. Excited States
   - Generalized pencil of functions
   - **Simultaneous multi-state fit models**
4. Results + chiral and continuum extrapolations

In collaboration with:

Tim Harris, Harvey Meyer, Georg von Hippel, Jonas Wilhelm, Hartmut Wittig

Introduction

We consider nucleon forward matrix elements

$$\left\langle N(p',s')\,|\mathcal{O}|\,N(p,s)\right\rangle . \tag{1}$$

"Standard" nucleon charges (g_A, g_T, g_S) require **local** operators: $\mathcal{O} = \bar{q}\gamma_\mu\gamma_5 q$, $\bar{q} i\sigma_{\mu\nu} q$, $\bar{q} q$.

- Can be computed directly at zero momentum (unlike magnetic moment $\mu_N = G_M(0)$).
- Consider only observables with $Q^2 = 0$.

Nucleon quark momentum fraction is the first momentum of unpolarized quark distribution:

$$\langle x \rangle_q = \int_0^1 x \cdot [q(x) + \bar{q}(x)] . \tag{2}$$

Similarly: First momenta for helicity (Δq) and transversity (δq) distributions.

On the lattice they require one-derivative, **dimension-four** operators:

$$\mathcal{O}^{vD}_{\mu\nu} = \bar{q}\gamma_{\{\mu}\overleftrightarrow{D}_{\nu\}}\, q\,, \quad \mathcal{O}^{aD}_{\mu\nu} = \bar{q}\gamma_{\{\mu}\gamma_5\overleftrightarrow{D}_{\nu\}}\, q\,, \quad \mathcal{O}^{tD}_{\mu\nu\rho} = \bar{q}\sigma_{[\mu\{\nu}\overleftrightarrow{D}_{\rho\}}\, q\,, \tag{3}$$

where

- $\{\ldots\}$ denotes symmetrization over indices and subtraction of the trace,
- $[\ldots]$ denotes anti-symmetrization over indices.

Matrix elements, FF decomposition and ratios

Can compute forward nucleon matrix elements in lattice QCD, but extracting nucleon structure information requires additional steps:

- For e.g. $\mathcal{O}^{vD}_{\mu\nu}$ the FF decomposition of the nucleon matrix element reads

$$\left\langle N(p',s') \left| \mathcal{O}^{vD}_{\mu\nu} \right| N(p,s) \right\rangle = \bar{u}(p',s') \left[\gamma_{\{\mu} \bar{P}_{\nu\}} A_{20}(Q^2) - \frac{\sigma_{\{\mu\alpha} Q_\alpha Q_{\nu\}}}{2m_N} B_{20}(Q^2) + \frac{1}{m_N} Q_{\{\mu} Q_{\nu\}} C_{20}(Q^2) \right] u(p,s) \,. \tag{4}$$

- Spin-projecting with $\Gamma_0 = \frac{1}{2}(1+\gamma_0)$ and $\Gamma_z = \Gamma_0(1+i\gamma_5\gamma_3)$ and considering zero momentum transfer $Q=0$ we compute the ratio

$$R^{vD}(t_f,t,t_i) \equiv \frac{C^{\mu\mu}_{3\mathrm{pt}}(\vec{q}=0,t_f,t_i,t;\Gamma_z)}{C_{2\mathrm{pt}}(\vec{q}=0,t_f-t_i;\Gamma_0)} \to \begin{cases} -\frac{3}{4} m \langle x \rangle_{u\pm d} & \text{for } \mu = 0 \\ +\frac{1}{4} m \langle x \rangle_{u\pm d} & \text{for } \mu = 1,2,3 \end{cases} , \tag{5}$$

  for $t_f - t \gg 1$, $t - t_i \gg 1$ and where $\langle x \rangle_{u\pm d} \equiv A_{20}(0)$.

- In practice $t_{\mathrm{sep}} \equiv t_f - t_i \lesssim 1.5\,\mathrm{fm}$:

  ⇒ **Ground state convergence not guaranteed, fitting the ratio ("plateau method") not good enough...**

Similar relations hold for $\mathcal{O}^{aD}_{\mu\nu}$, $\mathcal{O}^{tD}_{\mu\nu\rho}$: *Phys. Lett. B594 (2004) 164-170*

$$R^{aD}(t_f, t, t_i) \to -\frac{i}{2} m \langle x \rangle_{\pm u \Delta \pm d} \quad \text{for } \mu = 3, \nu = 0\,, \tag{6}$$

$$R^{tD}(t_f, t, t_i) \to +\frac{i}{4} m \left(2\delta_{0\rho} - \delta_{0\mu} - \delta_{0\nu}\right) \langle x \rangle_{\pm u \delta \pm d} \quad \neq 0 \text{ for e.g. } \mu = 0, \nu = 1, \rho = 2\,. \tag{7}$$

and for the local operators.

g_A and $\langle x \rangle$ are closely related to the nucleon spin structure:

$$J_N = \sum_q \underbrace{\left(\frac{1}{2}\Delta q + L_q\right)}_{\equiv J_q} + J_g\,. \tag{8}$$

Phys. Rev. Lett. 78, 610 (1997)

- $\Delta q = g_A^q$ is the quark spin contribution.
- The total quark angular momentum J_q is related to the second Mellin-moment of the unpolarized nucleon PDF

$$J_q = \frac{1}{2}\left(A^q_{20}(0) + B^q_{20}(0)\right), \qquad A^q_{20}(0) = \langle x \rangle_q\,. \tag{9}$$

- $B^q_{20}(0)$ cannot be obtained directly at $Q^2 = 0$; needs extrapolation of GFF data
- (Very) recent lattice results by ETMC (2017), PNDME (2018).
- This talk: focus on extraction of (isovector) g_A^{u-d}, $\langle x \rangle_{u-d}$ and **treatment of excited states**.

Computation of 2pt and 3pt functions

We use the truncated solver method:

$$\langle \mathcal{O} \rangle = \langle \frac{1}{N_{LP}} \sum_{i=1}^{N_{LP}} \mathcal{O}_n^{LP} \rangle + \langle \mathcal{O}_{\text{bias}} \rangle, \quad \mathcal{O}_{\text{bias}} = \frac{1}{N_{HP}} \sum_{i=1}^{N_{HP}} (\mathcal{O}_n^{HP} - \mathcal{O}_n^{LP}) \tag{10}$$

Comput.Phys.Commun. 181 (2010) 1570-1583
Phys.Rev. D91 (2015) no.11, 114511

Typically, per configuration:

- $N_{HP} = 1$ high-precision inversion(s)
- $N_{LP} = 16...48$ low-precision inversions

$\rightarrow$ **Gain of factor 2-3 in compute time**

- For 3pt functions we use sequential inversions through the sink, setting $p' = 0$.
- **Isovector matrix elements require only quark-connected 3pt functions**
- For isoscalar matrix elements we work on adding disconnected diagrams

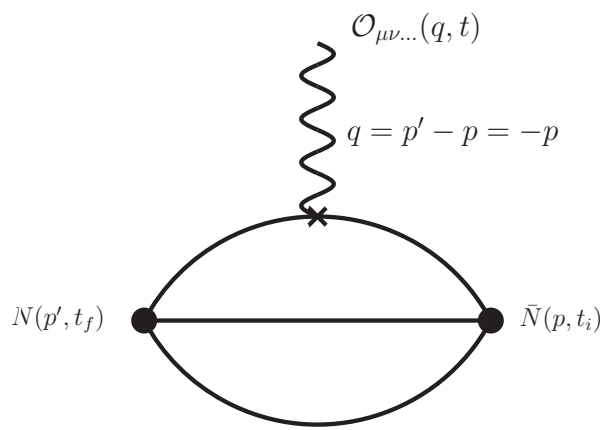

Lattice setup

To obtain physical results from lattice simulations one needs to:

- **Control discretization effects:**
  - Simulate at different (small) values of the lattice spacing a.
  - Perform continuum extrapolation.
  - We have simulations at four values of a ($0.049\,\mathrm{fm}$, $0.064\,\mathrm{fm}$, $0.076\,\mathrm{fm}$ and $0.086\,\mathrm{fm}$).
  - For some of the charges (g_A,g_S) exhibit only $\mathcal{O}(a^2)$ artifacts.
- **Correct for unphysical pion masses:**
  - Simulate at several pion masses.
  - Perform chiral extrapolation.
  - Our pion masses range from $\sim 200\,\mathrm{MeV}$ to $\sim 350\,\mathrm{MeV}$.
  - We will add an ensemble with physical light quark mass.
- **Control finite size effects:**
  - Simulate at large enough volumes.
  - We use ensembles with $M_\pi L \gtrsim 4$.

Gauge ensembles

ID	β	T/a	L/a	aM_π	M_π / GeV	$M_\pi L$	N_{HP}	N_{LP}	twist-2	t_{sep} / fm
C101	3.40	96	48	0.0976(09)	0.223(3)	4.68	1908	15264	no	1.0, 1.2, 1.4
H102	3.40	96	32	0.1541(06)	0.352(4)	4.93	7988	0	no	1.0, 1.2, 1.4
H105	3.40	96	32	0.1219(10)	0.278(4)	3.90	4076	48912	yes	1.0, 1.2, 1.4
N401	3.46	128	48	0.1118(06)	0.289(4)	5.37	701	11216	yes	1.1, 1.2, 1.4, 1.5, 1.7
S400	3.46	128	32	0.1352(06)	0.350(4)	4.33	1725	27600	yes	1.1, 1.2, 1.4, 1.5, 1.7
D200	3.55	128	64	0.0661(03)	0.203(3)	4.23	1021	32672	yes	1.0, 1.2, 1.3, 1.4
N200	3.55	128	48	0.0920(03)	0.283(3)	4.42	1697	20364	yes	1.0, 1.2, 1.3, 1.4
N203	3.55	128	48	0.1130(02)	0.347(4)	5.42	1540	24640	yes	1.0, 1.2, 1.3, 1.4, 1.5
J303	3.70	192	64	0.0662(03)	0.262(3)	4.24	531	8496	yes	1.0, 1.1, 1.2, 1.3
N302	3.70	128	48	0.0891(03)	0.353(4)	4.28	1177	18832	yes	1.0, 1.1, 1.2, 1.3, 1.4

- $N_f = 2+1$ flavors of non-perturbatively improved Wilson clover fermions. *JHEP 1502 (2015) 043*
- Lüscher-Weisz gauge action *Commun.Math.Phys. 97 (1985)*
- Exceptional configurations are suppressed by a twisted mass regulator. *PoS LATTICE2008 (2008) 049*
- Generated with open boundary conditions in time. *Comput. Phys. Commun. 184 (2013)*
- Up to five source-sink separations; typically 1.0 fm to 1.4 fm.

Renormalization

Non-perturbative renormalization has been performed for the **three lower values of** β using the Rome-Southampton method:

β	Z_A	$Z_S^{\overline{\mathrm{MS}}}$	$Z_T^{\overline{\mathrm{MS}}}$	$Z_{v2a}^{\overline{\mathrm{MS}}}$	$Z_{v2b}^{\overline{\mathrm{MS}}}$	$Z_{r2a}^{\overline{\mathrm{MS}}}$	$Z_{r2b}^{\overline{\mathrm{MS}}}$	$Z_{h1a}^{\overline{\mathrm{MS}}}$	$Z_{h1b}^{\overline{\mathrm{MS}}}$
3.40	0.75328(21)	0.6506(19)	0.83359(12)	1.10492(7)	1.11662(6)	1.09696(7)	1.13422(07)	1.13805(7)	1.14732(07)
3.46	0.76043(17)	0.6290(17)	0.84754(08)	1.12233(4)	1.12868(4)	1.11514(4)	1.14753(04)	1.15746(4)	1.16673(04)
3.55	0.77060(14)	0.6129(14)	0.86656(07)	1.15690(4)	1.16072(4)	1.15014(5)	1.17916(05)	1.19552(5)	1.20471(05)
3.70	0.78788(18)	0.5758(16)	0.89943(12)	1.21051(8)	1.20710(7)	1.20472(9)	1.22591(10)	1.25457(9)	1.26365(10)

- Each of the derivative operators falls into two different irreps of $H(4)$. *Phys. Rev. D54 (1996) 5705* *Phys. Rev. D82 (2010) 114511*
- Matrix elements agree in the continuum limit.
- Blue irreps are required for the *vD*, *aD* and *tD* operators used in our calculation.
- Values at $\beta = 3.70$ extrapolated.
- (Relative) effects of renormalization are of similar size as found in other studies.
- Errors are statistical only; irrelevant for total error budget.
- Results are given in $\overline{\mathrm{MS}}$ at $Q^2 = 4\,\mathrm{GeV}^2$.

Excited states

Nucleon structure calculations are notoriously hampered by **excited state contaminations**:

- Need large t_{sep} for plateau method $\rightarrow$ signal-to-noise problem
- Almost all lattice determinations of g_A approach experimental value from below (at few percent level).

- Situation more severe for less well-known observables, e.g. $\langle x \rangle_{u-d}$
- Very different systematics
- Several results at physical quark masses, but chiral + continuum extrapolation unclear
- Lattice seems to favor larger values for $\langle x \rangle_{u-d}$ ...

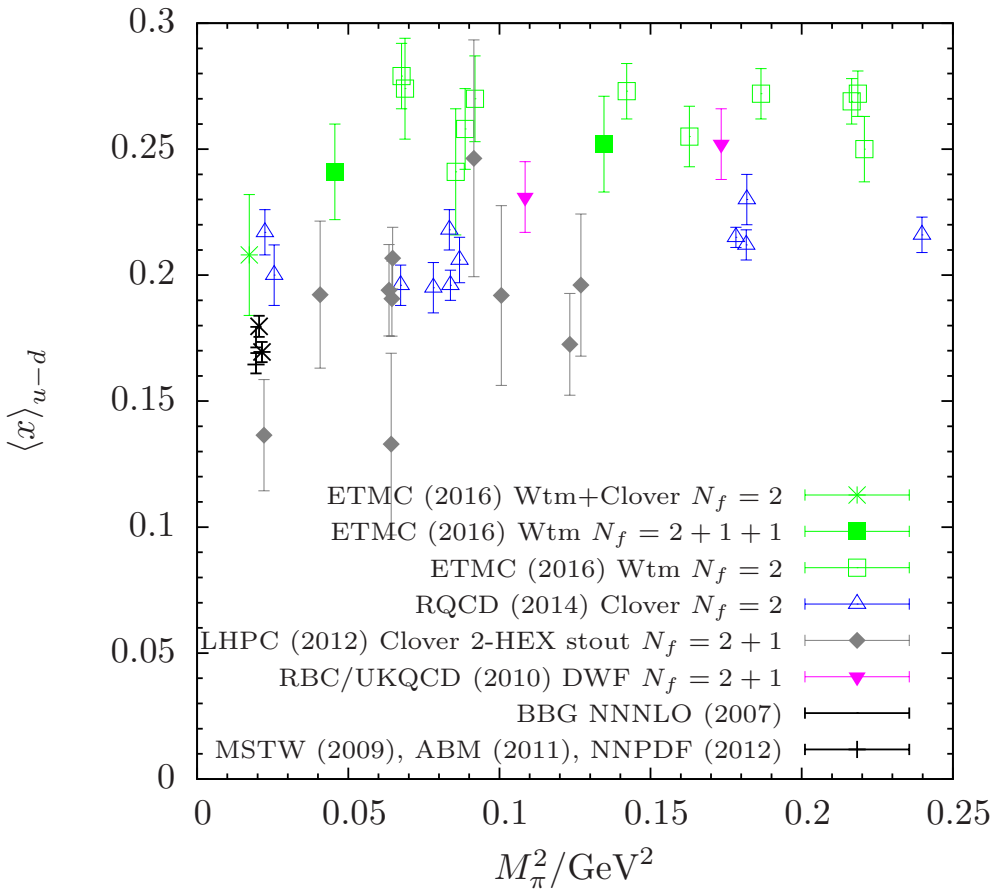

Excited states

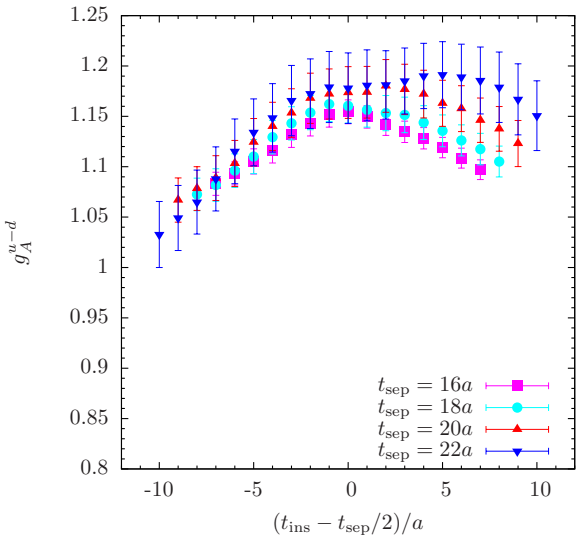

g_A on D200

($M_\pi = 203\ \mathrm{MeV}$, $a = 0.064\ \mathrm{fm}$)

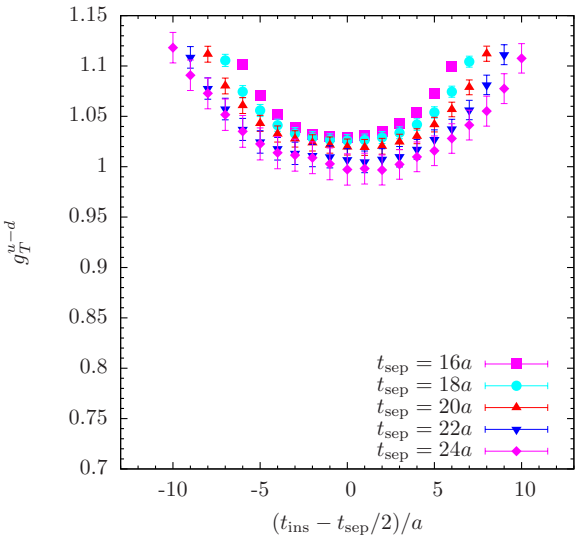

g_T on N203

($M_\pi = 347\ \mathrm{MeV}$, $a = 0.064\ \mathrm{fm}$)

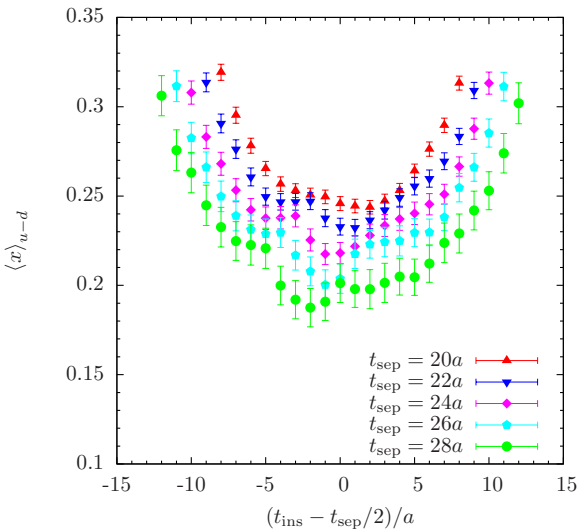

$\langle x \rangle_{u-d}$ on N302

($M_\pi = 353\ \mathrm{MeV}$, $a = 0.049\ \mathrm{fm}$)

- We observe excited state contamination on all ensembles.
- Contamination generally worse for twist-2 (and at smaller pion masses).
- No ground state convergence observed up to $t_{\rm sep} = 1.5\,\mathrm{fm}$.

Summation method

Straightforward approach to reduce excited state-contamination

$$\sum_{t=t_i+2}^{t_f-2} R(t_f, t, t_i) \sim c + t_f \cdot \mathcal{M}_0 + \mathcal{O}\left(e^{-\Delta E(t_f - t_i)}\right)$$

Nucl. Phys. B293 (1987) 420

- Only linear fit required to obtain $\mathcal{M}_0$.
- Leading excited state more strongly suppressed by $t_{\text{sep}} = t_f - t_i$
- But large errors
- Typically dominated by smallest t_{sep}
- Useful as Xcheck.

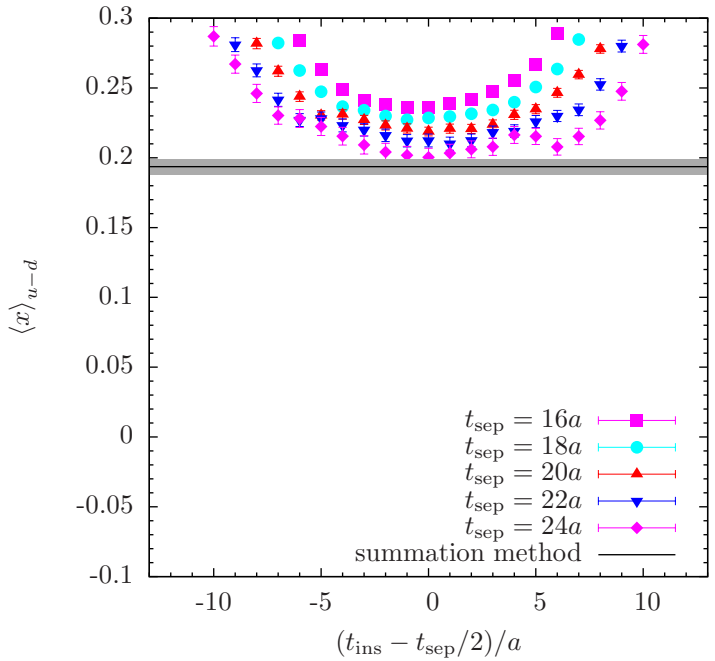

Plateaux and summation method on N203 ($V = 128 \times 48^3$, $M_\pi = 345$ MeV, $a = 0.064$ fm)

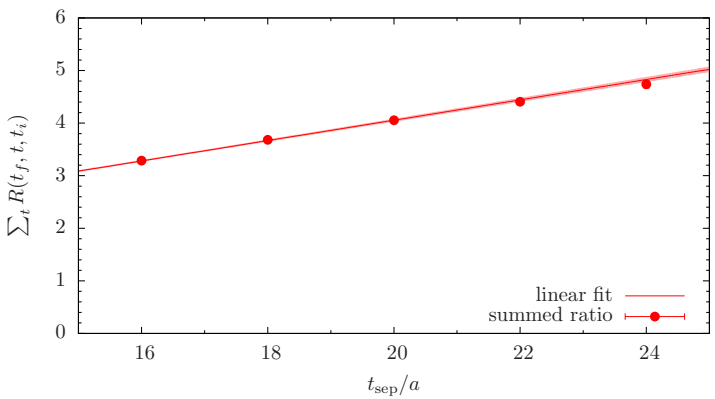

Linear fit for summation method on N203

Generalized pencil-of-functions (GPOF)

Instead of extending the actual operator basis, make use of the fact that

$$\mathcal{O}_{\Delta t}(t) \equiv \mathcal{O}(t+\Delta t) = \exp(H\Delta t)\mathcal{O}(t)\exp(-H\Delta t)\,, \tag{11}$$

is a new, and **linearly independent** interpolating operator. *AIP Conf.Proc. 1374 (2011)*

For 2pt functions construct $(n+1)\times(n+1)$ correlation function matrix for fixed Δt, $t \equiv t_f - t_i$:

$$\mathcal{C}_{2\mathrm{pt}}(t) = \begin{pmatrix} \langle \mathcal{O}_{0\cdot\Delta t}(t_f)\mathcal{O}^\dagger(t_i)\rangle & \dots & \langle \mathcal{O}_{0\cdot\Delta t}(t_f)\mathcal{O}^\dagger_{n\cdot\Delta t}(t_i)\rangle \\ \vdots & \ddots & \vdots \\ \langle \mathcal{O}_{n\cdot\Delta t}(t_f)\mathcal{O}^\dagger(t_i)\rangle & \dots & \langle \mathcal{O}_{n\cdot\Delta t}(t_f)\mathcal{O}^\dagger_{n\cdot\Delta t}(t_i)\rangle \end{pmatrix} = \begin{pmatrix} C_{2\mathrm{pt}}(t) & \dots & C_{2\mathrm{pt}}(t+n\cdot\Delta t) \\ \vdots & \ddots & \vdots \\ C_{2\mathrm{pt}}(t+n\cdot\Delta t) & \dots & C_{2\mathrm{pt}}(t+2n\cdot\Delta t) \end{pmatrix}. \tag{12}$$

$\rightarrow$ GEVP gives eigenvalues $\lambda^{(n)}(t,t_0)$ and matrix of eigenvectors $V \equiv (\vec{v}^0(t,t_0),\dots,\vec{v}^n(t,t_0))$.

Similarly, for 3pt functions:

$$\mathcal{C}_{3\mathrm{pt}}(t_f,t,t_i) = \begin{pmatrix} C(t_f,t,t_i) & \dots & C(t_f+n\cdot\Delta,t+n\cdot\Delta t,t_i) \\ \vdots & \ddots & \vdots \\ C(t_f+n\cdot\Delta t,t,t_i) & \dots & C(t_f+2n\cdot\Delta t,t+n\cdot\Delta t,t_i)\,. \end{pmatrix} \tag{13}$$

$\rightarrow$ **This matrix is not symmetric but can be diagonalized using V from 2pt case.**

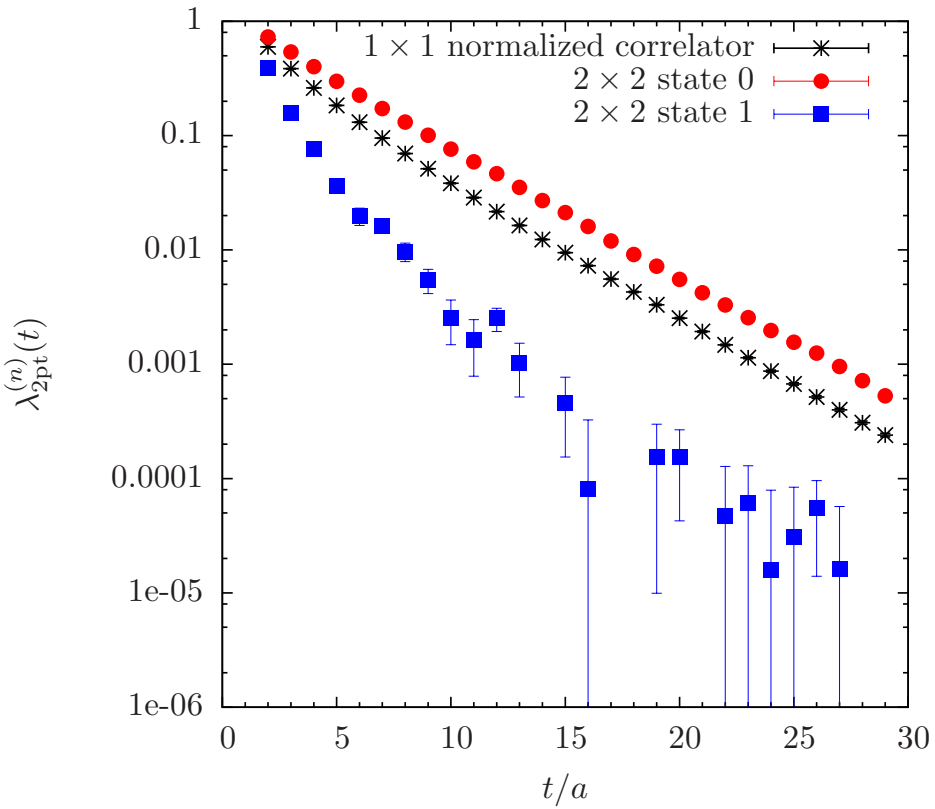

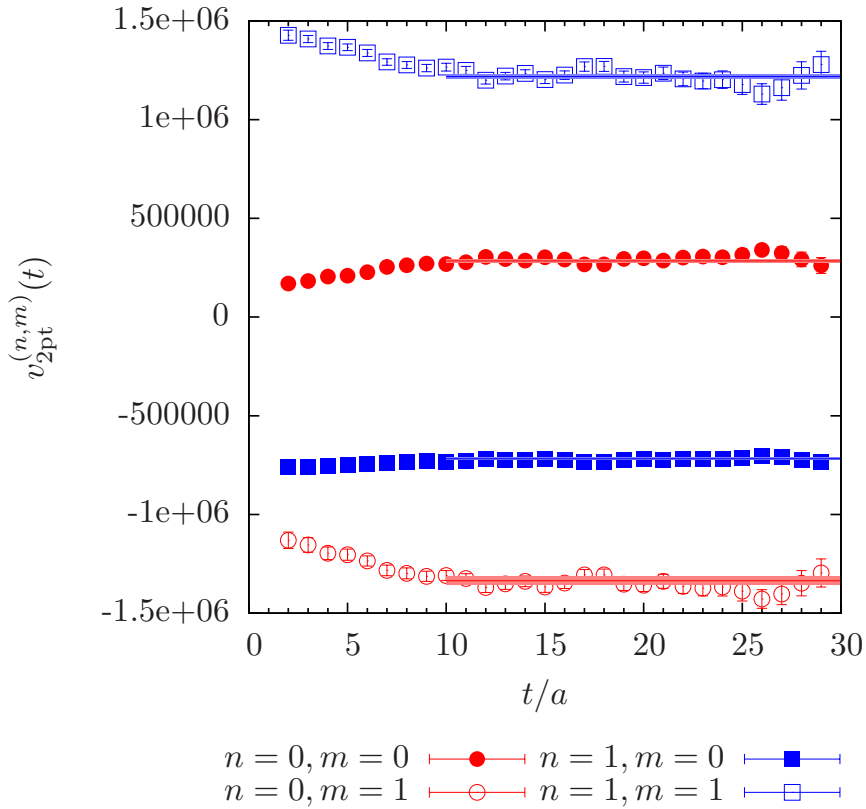

Eigenvalues and eigenvectors for J303 ($V = 192 \times 64^3$, $M_\pi = 262$ MeV, $a = 0.049$ fm)

- Clear reduction of excited states for ground state principal correlator from 2×2 GEVP.
- Stat. err. on nucleon mass reduced by $\mathcal{O}(50\%)$.
- Some residual excited state effects remains (as expected).
- Fits to eigenvectors are stable; typically $\chi^2_{\mathrm{red}} \approx 1$.
- Actual choice of fit range has little impact on final result.

General procedure (sample-wise):

1. Solve GEVP for corresponding 2pt problem.
2. Fit eigenvectors in plateau region $\rightarrow V$ (time-independent)
3. Diagonalize $\mathcal{C}_{3\mathrm{pt}}(t_f, t, t_i)$:

$$\mathcal{C}_{3\mathrm{pt}}(t_f, t, t_i) \rightarrow V^T \mathcal{C}_{3\mathrm{pt}}(t_f, t, t_i) V \equiv \Lambda_{3\mathrm{pt}}(t_f, t, t_i) = \mathrm{diag}(\Lambda^{(0)}, ..., \Lambda^{(n)})(t_f, t, t_i)\,. \tag{14}$$

4. Replace "standard" ratio by new, optimized ratio

$$\frac{C_{3\mathrm{pt}}(\vec{q}=0, t_f, t_i, t; \Gamma_z)}{C_{2\mathrm{pt}}(\vec{q}=0, t_f - t_i; \Gamma_0)} \rightarrow \frac{\Lambda^{(0)}_{3\mathrm{pt}}(\vec{q}=0, t_f, t_i, t; \Gamma_z)}{\lambda^{(0)}_{2\mathrm{pt}}(\vec{q}=0, t_f - t_i; \Gamma_0)}\,. \tag{15}$$

5. Proceed with remaining analysis in the usual way...

Advantages:

- Method is straightforward to implement and does not require model assumptions.
- Uses existing data.
- Errors usually smaller than summation method.

A few restrictions in practice:

- We always have $t_i = 0$ and three up to five values for t_f.
- Need $n+1$ equidistant values of $t_f - t_i$ to build an $n \times n$ 3pt function matrix.

$\Rightarrow$ We are mostly restricted to 2×2 problems.

- t_f values are spaced by $\Delta t = 2a$ (e.g. $t_f/a = 16, 18, 20, \ldots$).

$\Rightarrow$ We are mostly restricted to $\Delta t = 2a$ in the operator construction for the 3pt case.

- Excited state removal not expected to be perfect for 2x2 GPOF
- For too many operators GPOF tends to become degenerate / singular

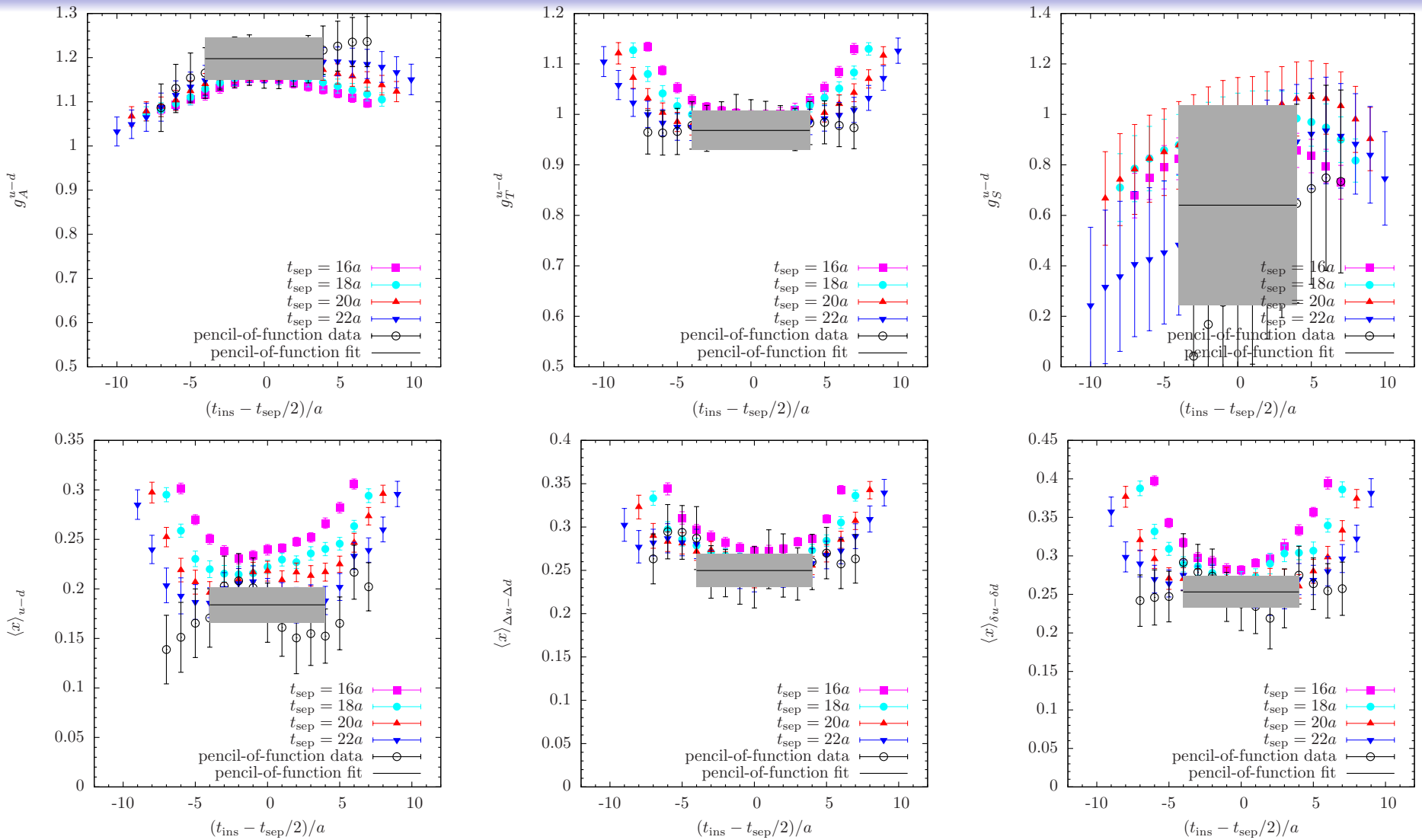

- GPOF results from the three largest values of t_{sep} on D200 ($M_\pi = 203\,\mathrm{MeV}$, $a = 0.064\,\mathrm{fm}$)
- On average smaller errors than summation method, even for using largest values of t_{sep}
- Data points highly correlated!

(Simultaneous) Multi-state fits

The effective charge / formfactor $R^{\mathcal{O}}(t_f, t, t_i, Q^2)$ can be described by a tower of states ($t_i = 0$)

$$R^{\mathcal{O}}(t_f, t, Q^2) = G_{\mathcal{O}}(Q^2) + \sum_n \Big(a_n^{\mathcal{O}}(Q^2) e^{-\Delta_n t} + b_n^{\mathcal{O}}(Q^2) e^{-\Delta'_n (t_f - t)} + c_n^{\mathcal{O}}(Q^2) e^{-\Delta'_k t_f - (\Delta_k - \Delta'_k) t} \Big) . \tag{16}$$

- $G_{\mathcal{O}}(Q^2)$ denotes the actual form factor,
- Δ_n, Δ'_n are energy gaps,
- $a_n^{\mathcal{O}}(Q^2)$, $b_n^{\mathcal{O}}(Q^2)$ and $c_n^{\mathcal{O}}(Q^2)$ denote amplitudes.

Assuming symmetric plateaux for $Q^2 = 0$ we have ($g_{\mathcal{O}} \equiv G_{\mathcal{O}}(0)$)

$$\boxed{R^{\mathcal{O}}(t_f, t, 0) = g_{\mathcal{O}} + \sum_n A_n^{\mathcal{O}} \left(e^{-\Delta_n t} + e^{-\Delta_n (t_f - t)} \right) + C_n^{\mathcal{O}} e^{-\Delta_n t_f} .} \tag{17}$$

- $A_n^{\mathcal{O}} \equiv a_n^{\mathcal{O}}(0) = b_n^{\mathcal{O}}(0)$, $C_n^{\mathcal{O}} \equiv c_n^{\mathcal{O}}(0)$ depend on observable $\mathcal{O}$.
- Δ_n are the same for different $\mathcal{O}$. $\rightarrow$ **simultaneous fits**
- Δ_0 is either fixed to lowest non-interacting level $2M_\pi$ or fitted from data.

Fit models

We investigated four different fit models:

1. Simultaneous fit to all observables; first gap fixed $\Delta_0 = 2M_\pi$, second gap free ("**FIT1**")
2. **Simultaneous fit to all observables; one free gap ("FIT2")**
3. Fit to individual observables; one free gap ("**FIT3**")
4. Fit to individual observables; one fixed gap $\Delta_0 = 2M_\pi$ ("**FIT4**")

Fits are subject to the following procedures / constraints:

- Data are explicitly symmetrized around $(t_f - t_i)/2 = t_f/2$.
- Fits use data from range $[t_{\text{start}}, t_f/2]$ for all available values of t_f.
- "Simultaneous" fits use local and twist-2 data if available, otherwise the three local charges
- **Final results from fits with same, fixed $M_\pi t_{\text{start}}$ for ALL ensembles.**
- **Can track convergence of free gap as function of $M_\pi t_{\text{start}} \rightarrow$ choice for fixing $M_\pi t_{\text{start}}$.**

Gap convergence for single observable fits (FIT3)

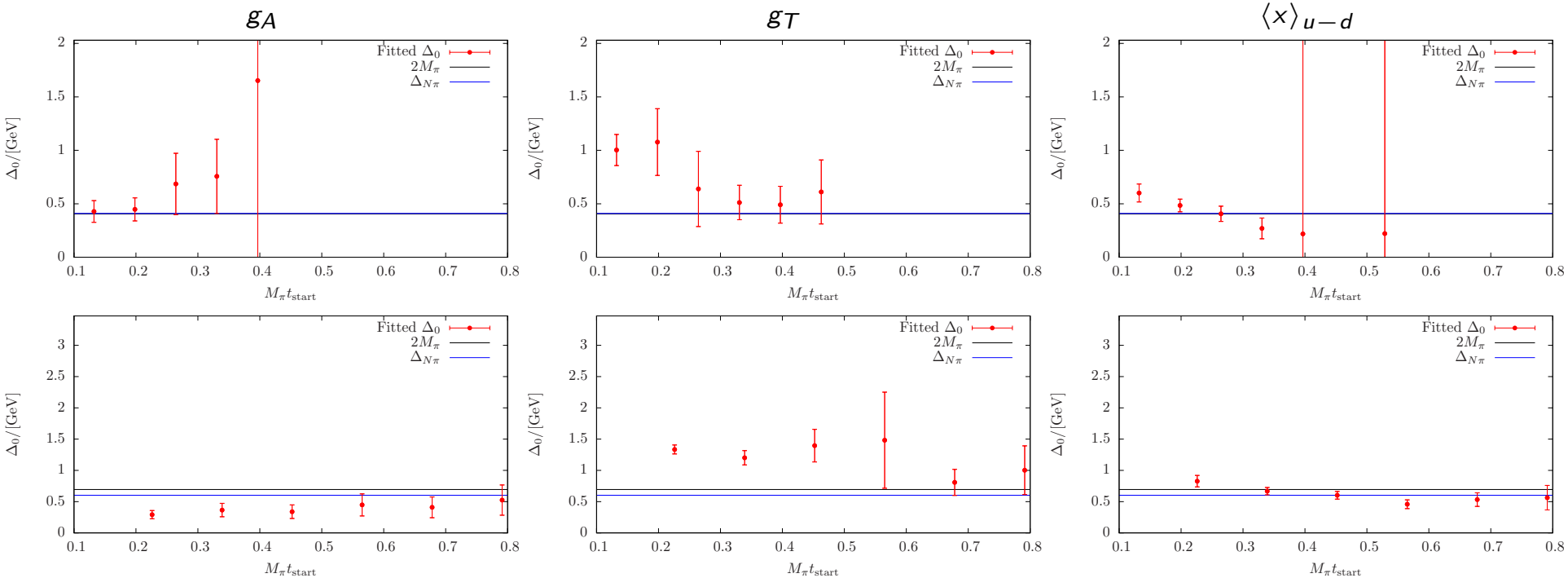

Upper row: D200 ($M_\pi = 203\,\mathrm{MeV}$, $a = 0.064\ \mathrm{fm}$), lower row: N203 ($M_\pi = 347\,\mathrm{MeV}$, $a = 0.064\ \mathrm{fm}$)

- Results from fitting $R^{\mathcal{O}}(t_f, t, 0) = g_{\mathcal{O}} + \sum_n A_n^{\mathcal{O}} \left(e^{-\Delta_n t} + e^{-\Delta_n (t_f - t)} \right)$ (one parameter less; term $\sim e^{-\Delta_n t_f}$ subleading).
- Signal for Δ_0 seems to approach $2M_\pi$, but often with large errors, unstable fits.
- Not yet useful for choosing global $M_\pi t_{\mathrm{start}}$ independent of observable, ensemble ...

Gap convergence for simultaneous fits (FIT2)

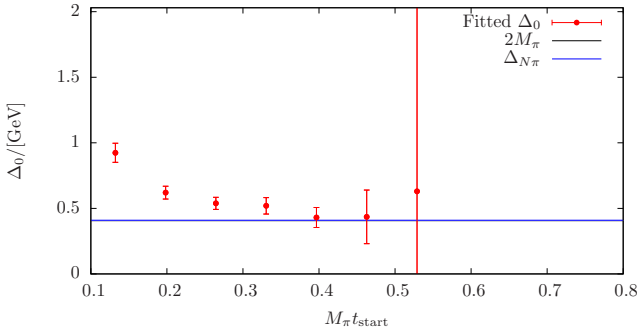

D200 ($M_\pi = 203\,\mathrm{MeV}$, $a = 0.064$ fm)

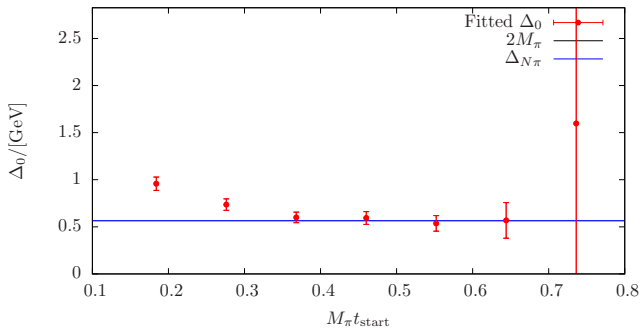

N200 ($M_\pi = 283\,\mathrm{MeV}$, $a = 0.064$ fm)

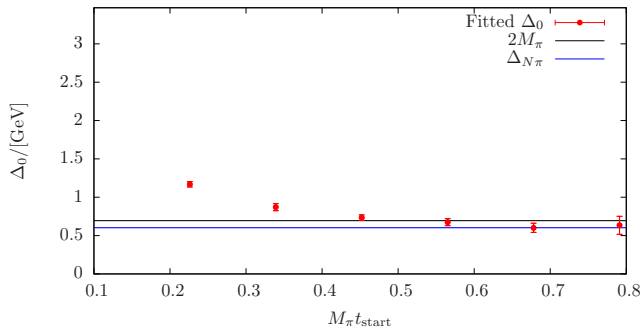

N203 ($M_\pi = 347\,\mathrm{MeV}$, $a = 0.064$ fm)

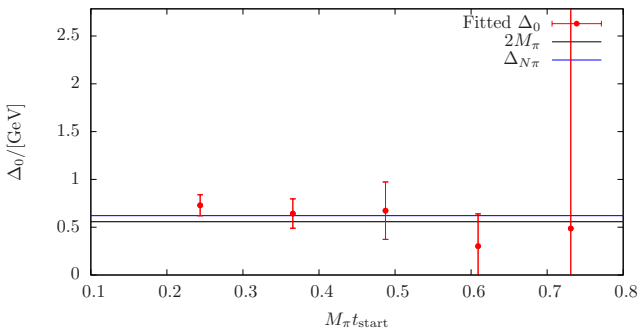

H105 ($M_\pi = 278\,\mathrm{MeV}$, $a = 0.086$ fm)

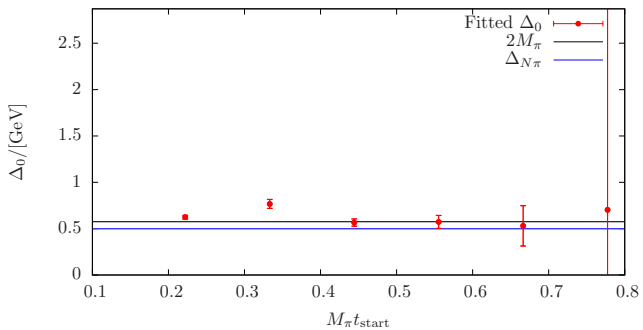

N401 ($M_\pi = 283\,\mathrm{MeV}$, $a = 0.076$ fm)

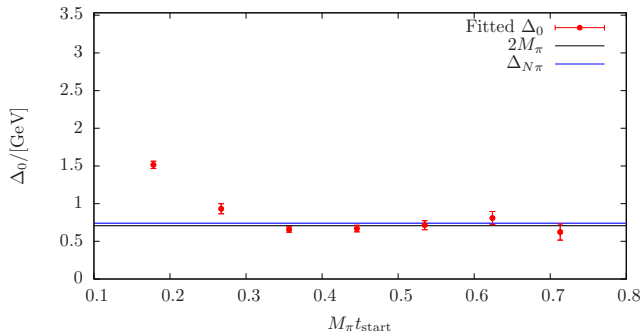

N302 ($M_\pi = 353\,\mathrm{MeV}$, $a = 0.049$ fm)

- Much more precise results for Δ_0 from simultaneous fits!
- Clear convergence on most ensembles; no observable dependence.
- Trade-off between statistical error and systematics due to excited states

→ **We choose $M_\pi t_{\mathrm{start}} = 0.4$ for our final analysis.**

Gap convergence for simultaneous fits (FIT2)

Adding term $\sim e^{-\Delta_n t_f}$ gaps become more noisy again (additional parameter):

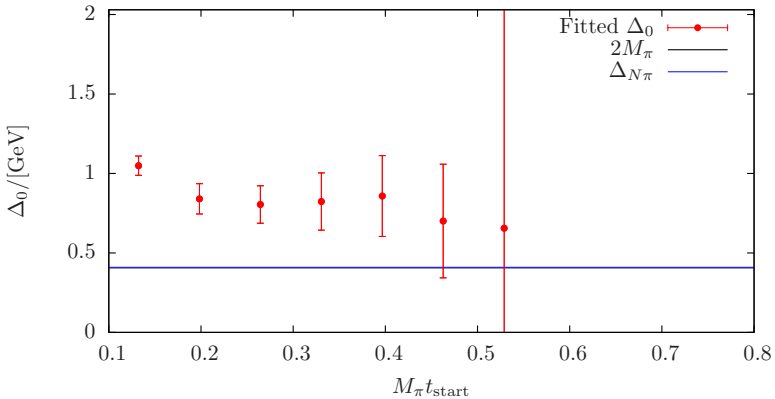

D200 ($M_\pi = 203\,\mathrm{MeV}$, $a = 0.064$ fm)

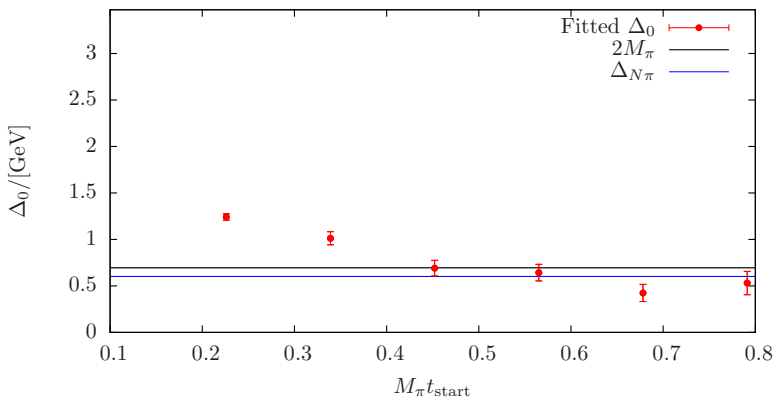

N203 ($M_\pi = 347\,\mathrm{MeV}$, $a = 0.064$ fm)

However, term $\sim e^{-\Delta_n t_f}$ not irrelevant:

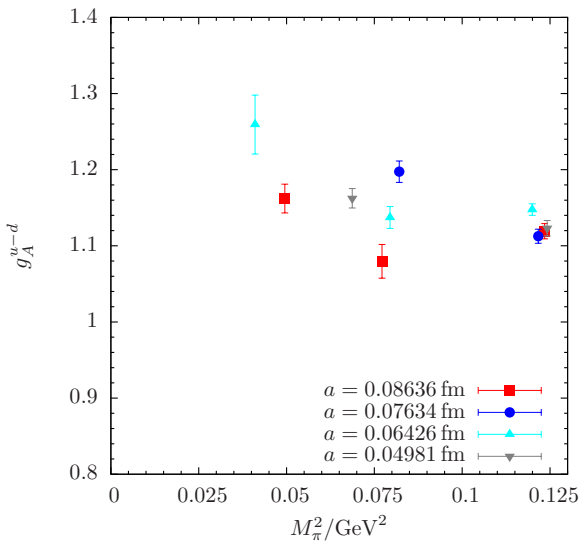

w/o term $\sim e^{-\Delta_n t_f}$

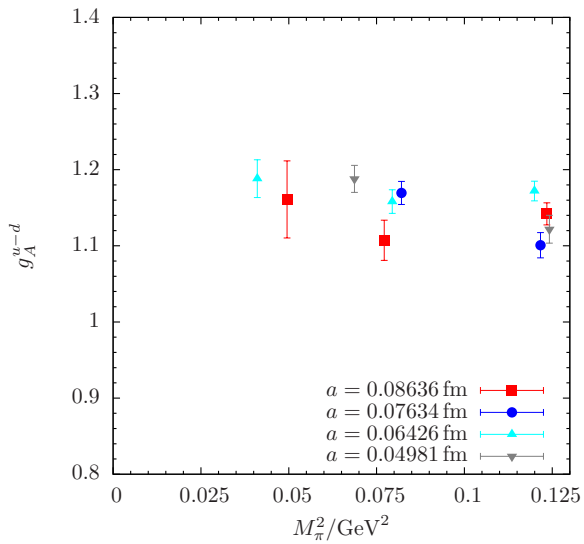

with term $\sim e^{-\Delta_n t_f}$

Fixed gap vs. free gap fit

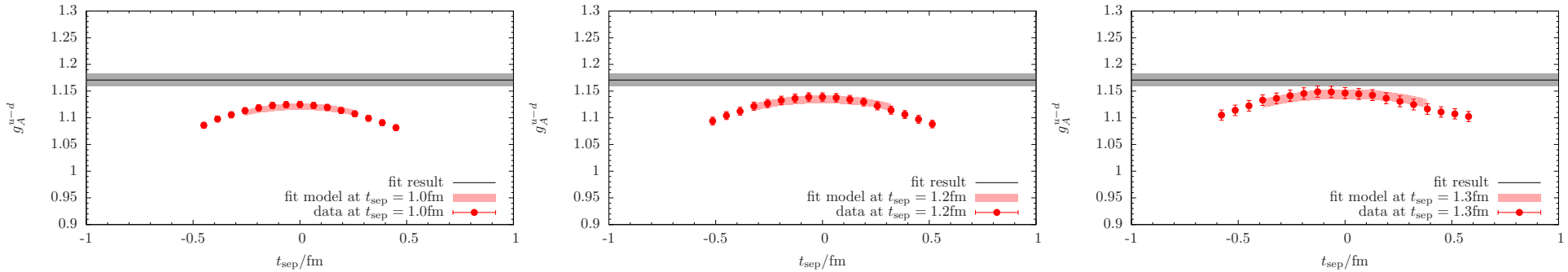

Fixed Δ_0 fit (FIT4) for g_A on N203 ($M_\pi = 347\,\mathrm{MeV}$, $a = 0.064$ fm) for three (out of five) values of $t_{\rm sep}$

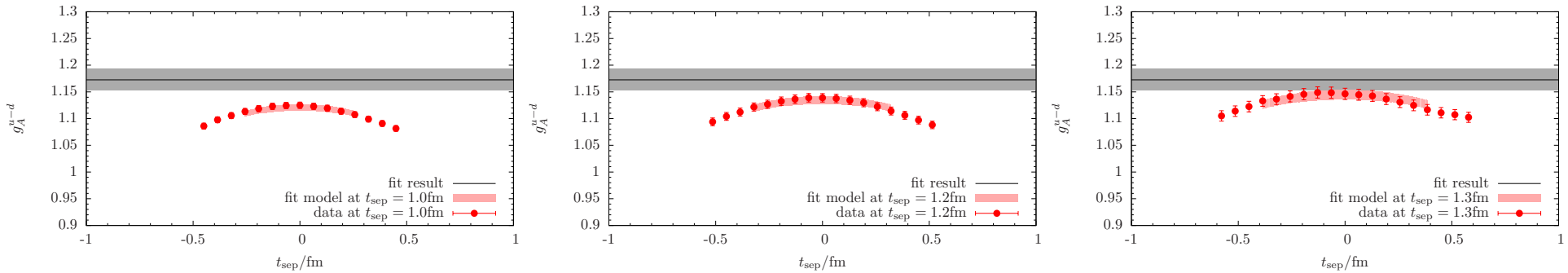

Free Δ_0 fit (FIT3) for g_A on N203 ($M_\pi = 347\,\mathrm{MeV}$, $a = 0.064$ fm) for three (out of five) values of $t_{\rm sep}$

- Fits are always simultaneous for ALL values of $t_{\rm tsep}$!
- High statistics ensemble for testing; heavy pion mass.
- Data well described by fit form (at chosen fit range).
- Final value agrees, but larger error for free Δ_0 (as expected).
- Single observable, free Δ_0 fits are often unstable for lower statistics / fitting few points.

Fixed gap vs. simultaneous (free gap) fit

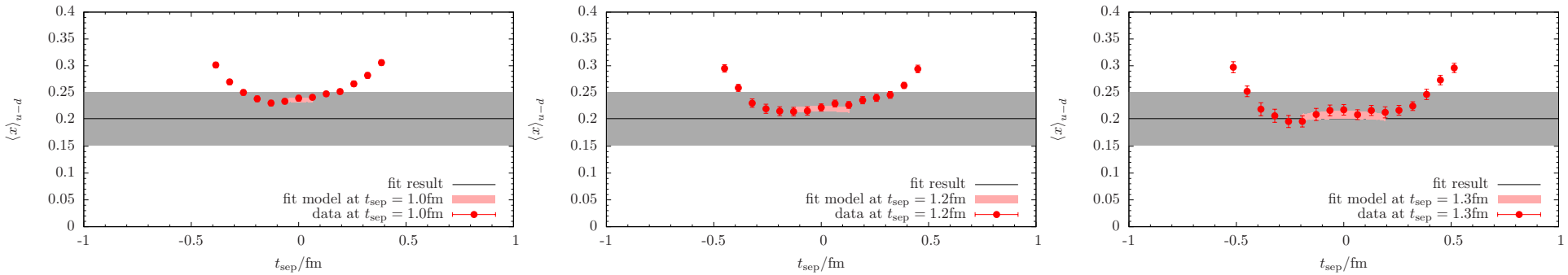

Fixed Δ_0 fit (FIT4) for $\langle x \rangle_{u-d}$ on D200 ($M_\pi = 203\,\mathrm{MeV}$, $a = 0.064$ fm) for three (out of four) values of t_{sep}

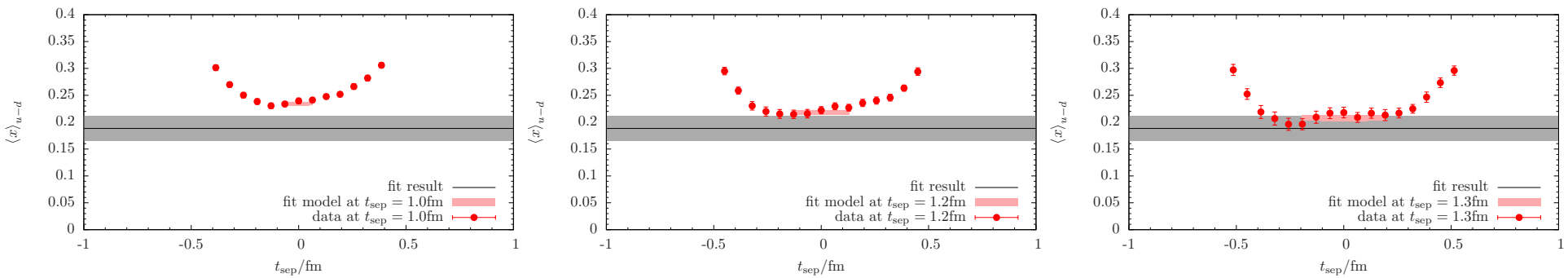

Simultaneous (free Δ_0) fit (FIT2). Results for $\langle x \rangle_{u-d}$ on D200 ($M_\pi = 203\,\mathrm{MeV}$, $a = 0.064$ fm)

- Fitting observables simultaneously results in much smaller errors.
- Often outperforms even fit with fixed Δ_0. (!)
- Much more stable than corresponding single observable fits.

Simultaneous fit results

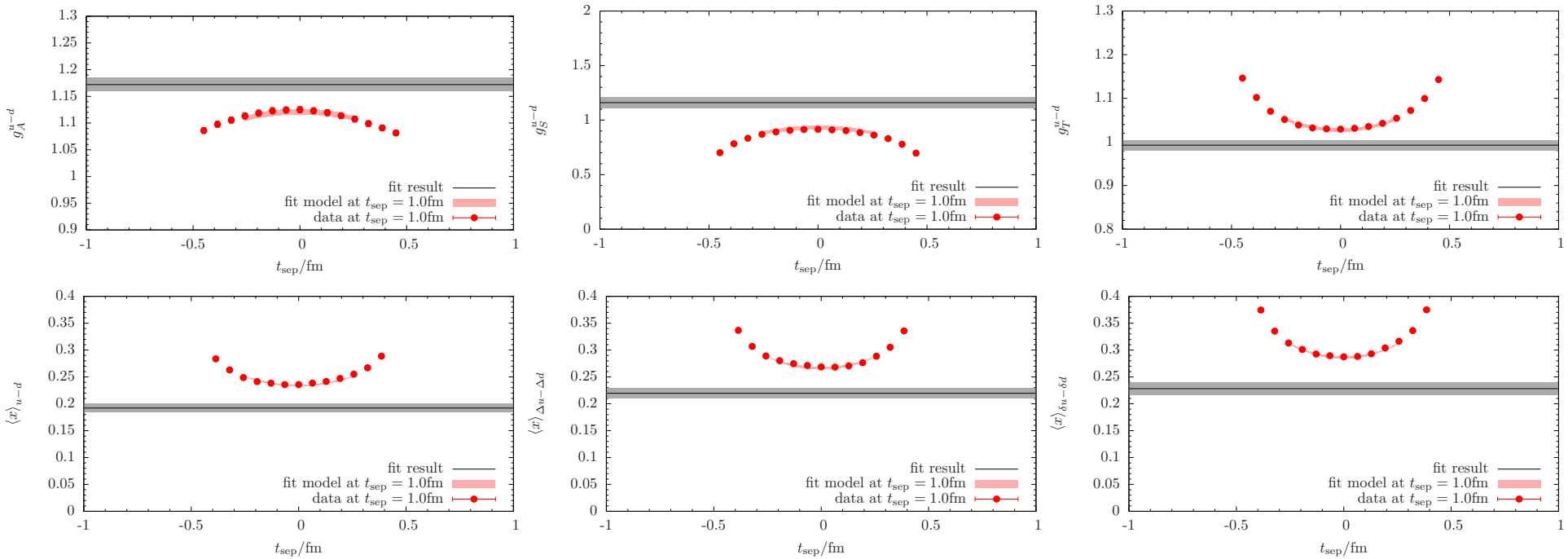

Results for all six observables from simultaneous (free Δ_0) fit on N203 ($M_\pi = 347\,\mathrm{MeV}$, $a = 0.064\ \mathrm{fm}$).

Results for $t_{\mathrm{sep}} = 16a$ are shown.

- Simultaneous fits describe data very well.
- Corrections can be sizable compared to plateau method at e.g. $t_{\mathrm{sep}} = 1.3\mathrm{fm}$
- Simultaneous fits supersede fixed gap / single observable fits (less ambiguity, better signal).

Simultaneous fit results

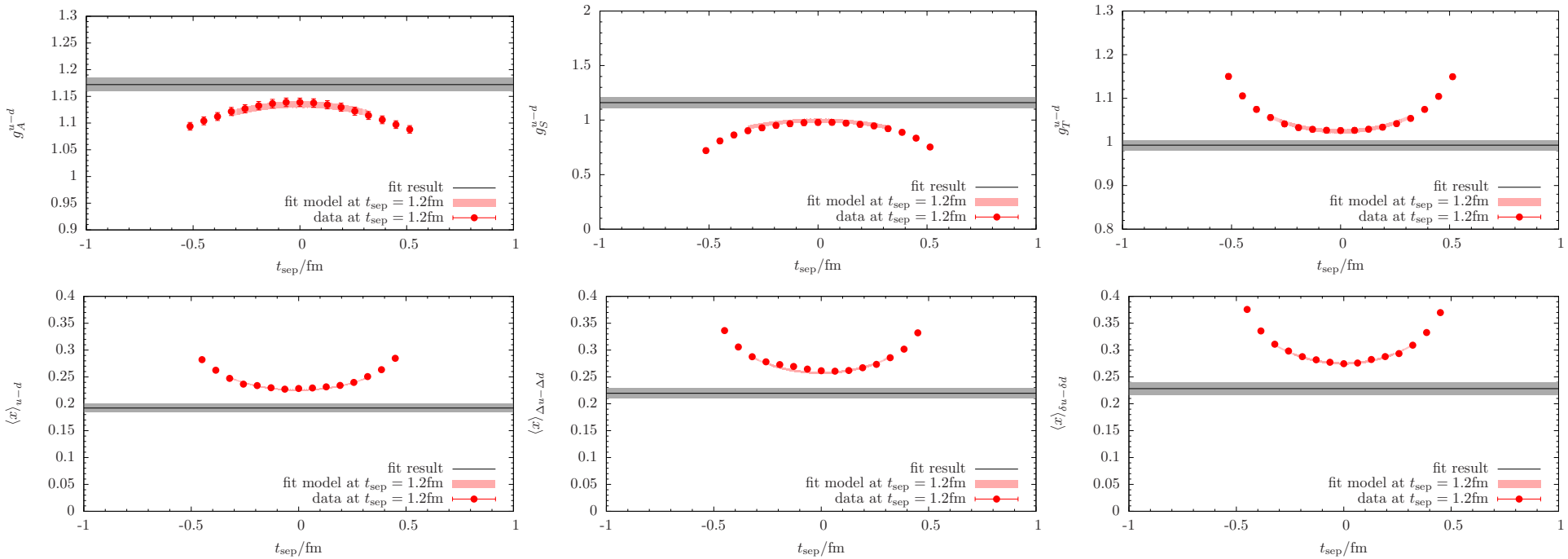

Results for all six observables from simultaneous (free Δ_0) fit on N203 ($M_\pi = 347\,\mathrm{MeV}$, $a = 0.064\ \mathrm{fm}$).

Results for $t_{\mathrm{sep}} = 18a$ are shown.

- Simultaneous fits describe data very well.
- Corrections can be sizable compared to plateau method at e.g. $t_{\mathrm{sep}} = 1.3\mathrm{fm}$
- Simultaneous fits supersede fixed gap / single observable fits (less ambiguity, better signal).

Simultaneous fit results

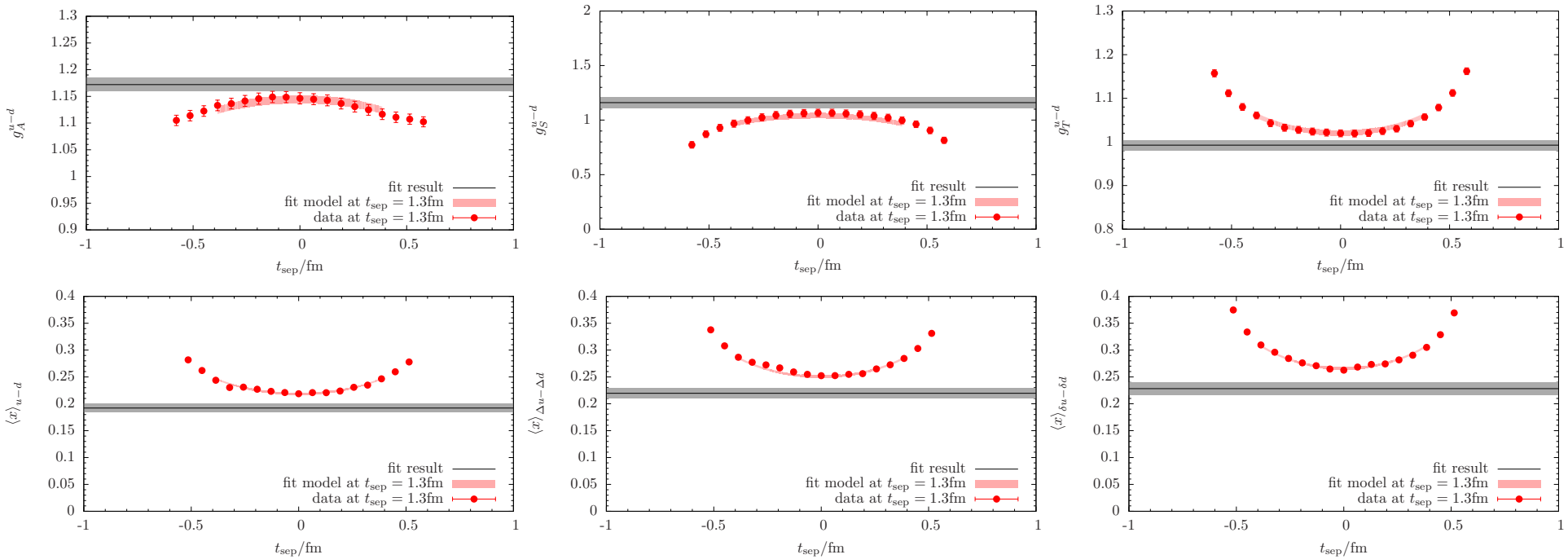

Results for all six observables from simultaneous (free Δ_0) fit on N203 ($M_\pi = 347\,\mathrm{MeV}$, $a = 0.064\ \mathrm{fm}$).

Results for $t_{\mathrm{sep}} = 20a$ are shown.

- Simultaneous fits describe data very well.
- Corrections can be sizable compared to plateau method at e.g. $t_{\mathrm{sep}} = 1.3\mathrm{fm}$
- Simultaneous fits supersede fixed gap / single observable fits (less ambiguity, better signal).

Simultaneous fit results

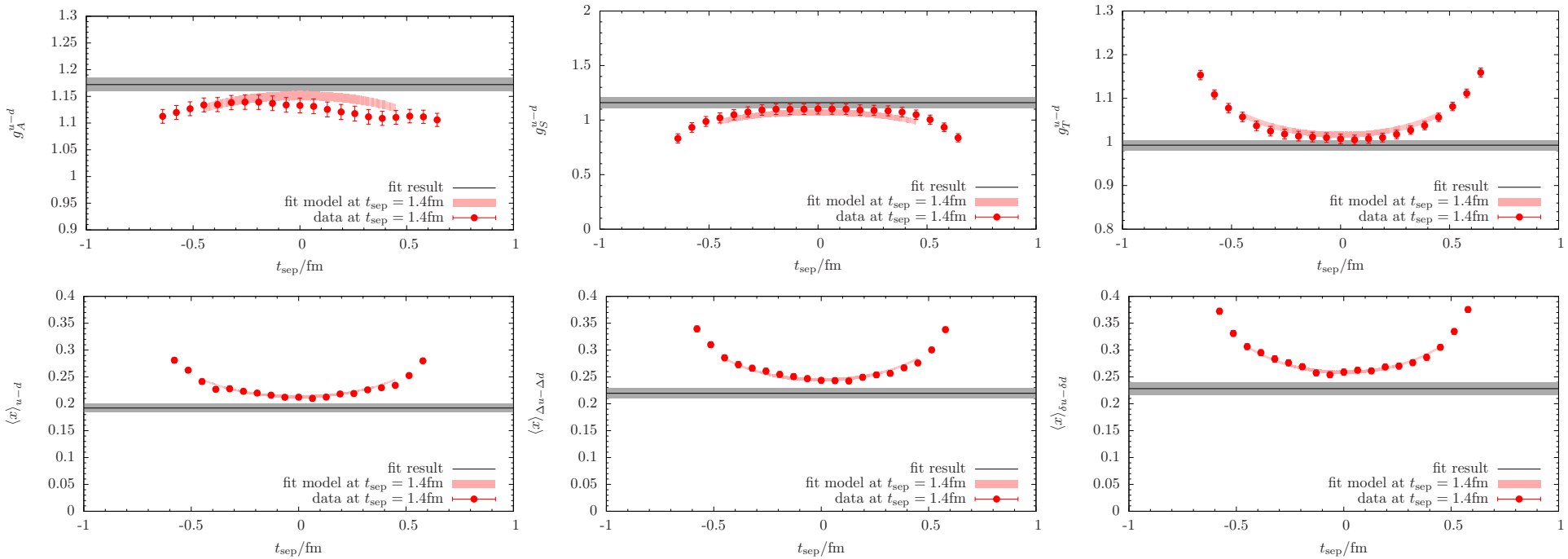

Results for all six observables from simultaneous (free Δ_0) fit on N203 ($M_\pi = 347\,\mathrm{MeV}$, $a = 0.064\ \mathrm{fm}$).

Results for $t_{\mathrm{sep}} = 22a$ are shown.

- Simultaneous fits describe data very well.
- Corrections can be sizable compared to plateau method at e.g. $t_{\mathrm{sep}} = 1.3\mathrm{fm}$
- Simultaneous fits supersede fixed gap / single observable fits (less ambiguity, better signal).

Simultaneous fit results

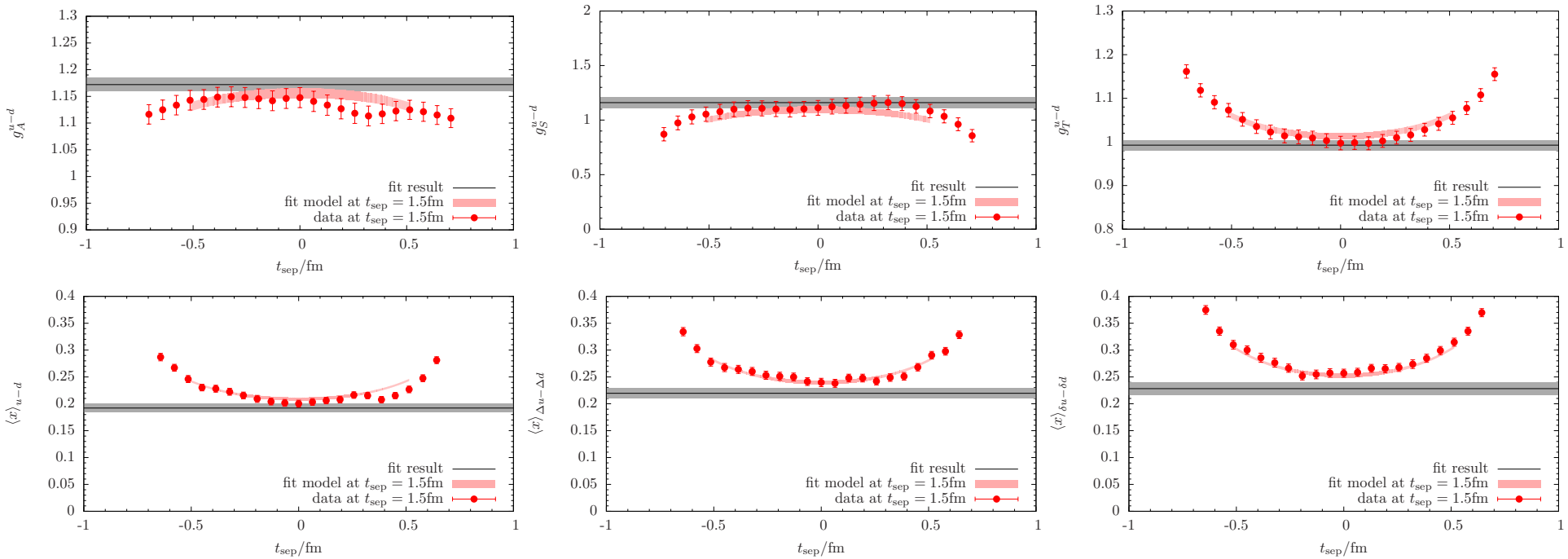

Results for all six observables from simultaneous (free Δ_0) fit on N203 ($M_\pi = 347\,\mathrm{MeV}$, $a = 0.064\ \mathrm{fm}$).

Results for $t_{\mathrm{sep}} = 24a$ are shown.

- Simultaneous fits describe data very well.
- Corrections can be sizable compared to plateau method at e.g. $t_{\mathrm{sep}} = 1.3\mathrm{fm}$
- Simultaneous fits supersede fixed gap / single observable fits (less ambiguity, better signal).

Overview of results from different methods

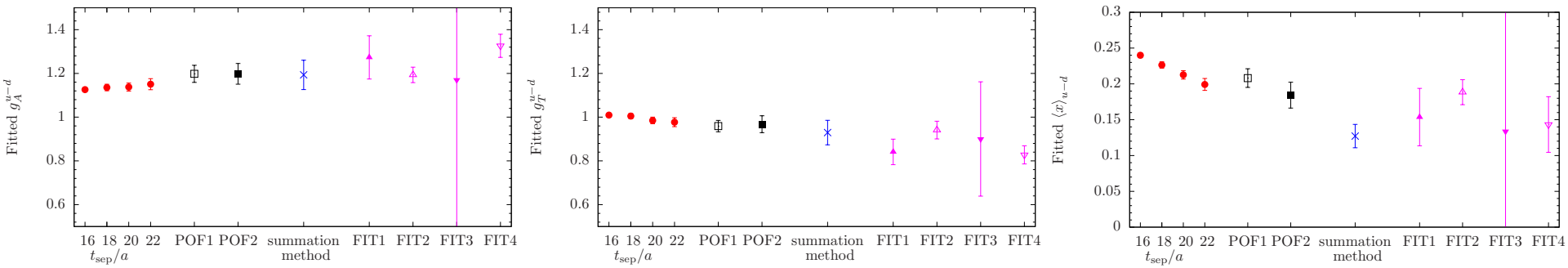

D200 ($M_\pi = 203\,\mathrm{MeV}$, $a = 0.064$ fm)

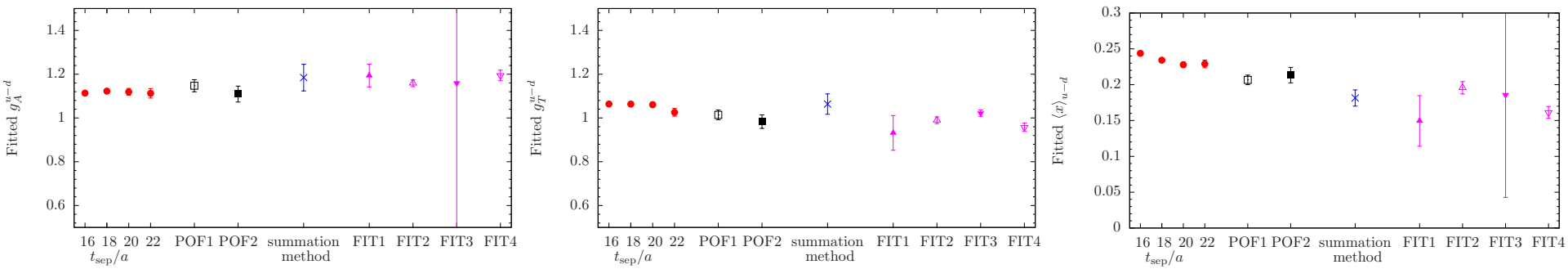

N200 ($M_\pi = 278\,\mathrm{MeV}$, $a = 0.064$ fm)

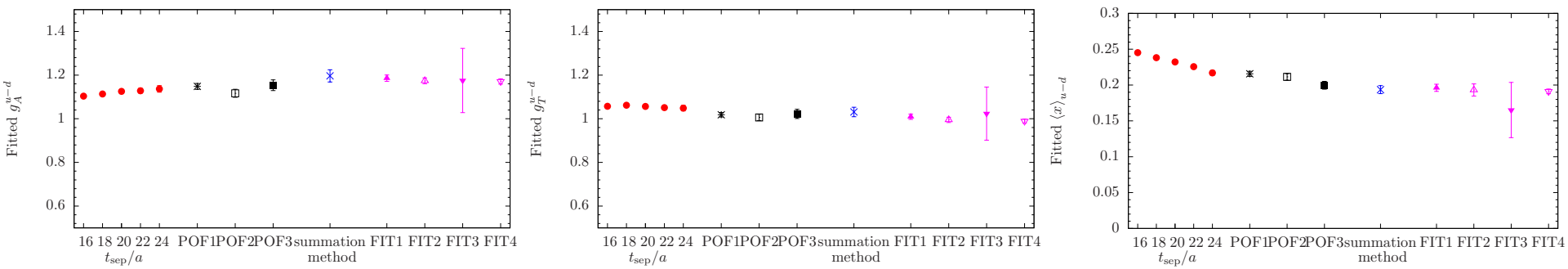

N203 ($M_\pi = 347\,\mathrm{MeV}$, $a = 0.064$ fm)

Overview of results for $\langle x \rangle_{u-d}$

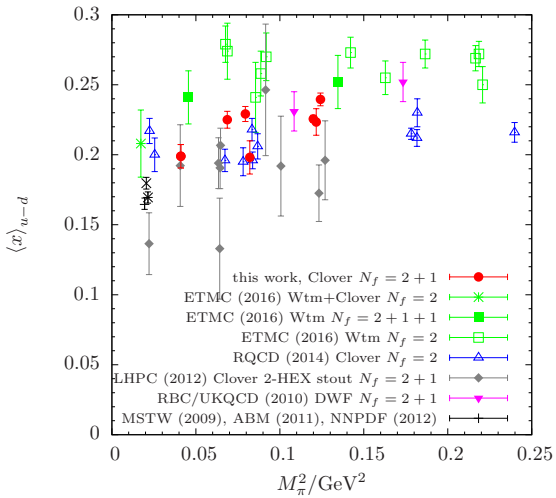

plateau method

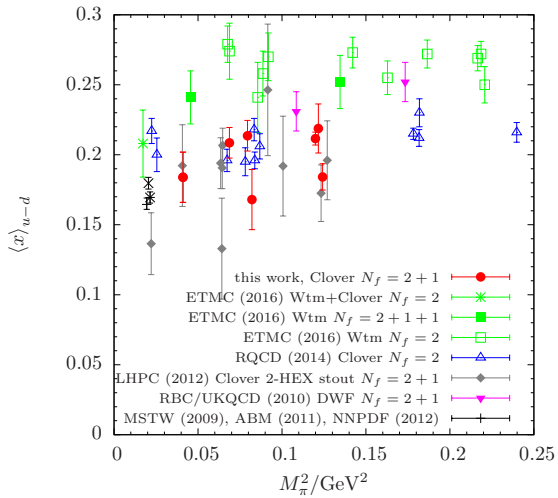

GPOF

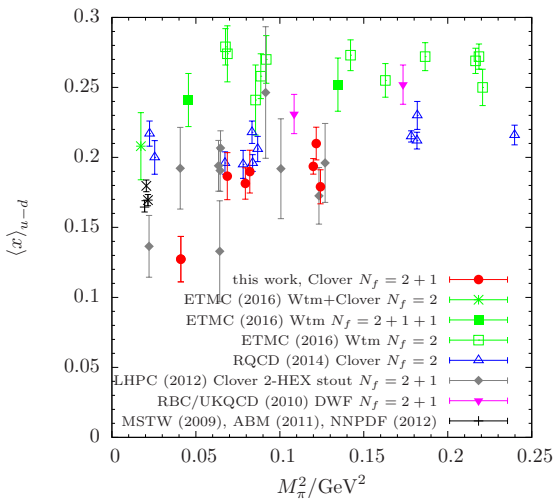

summation method

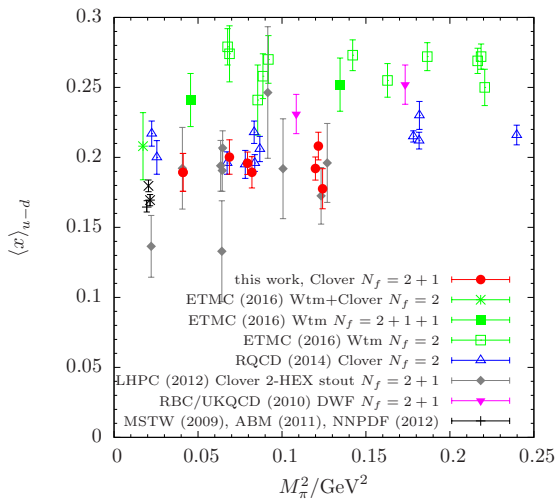

simultaneous fit

(all observables)

- Plateau method ($t_{\mathrm{sep}} \gtrsim 1.4\mathrm{fm}$) small errors and large values, as expected.
- GPOF systematically below plateau method, but non-negligible excited state contamination.
- Summation method compatible with simultaneous fit, but larger errors, unstable for most chiral ensemble.
- Results from simultaneous fit have smaller error, data less scattered than GPOF

Summary of methods

1. Plateau method
   - Smallest stat. error; non-negligible excited state contamination even for $t_{\mathrm{sep}} \gtrsim 1.4\mathrm{fm}$.
2. Summation method
   - Mostly compatible with fits, but large stat. errors.
3. GPOF
   - Usually results rather close to plateau method, although systematically different.
   - Larger stat. errors than plateau but smaller than summation method.
   - Current setup probably not optimal; three values of t_{sep} (with larger statistics) and $\Delta t = 4a$ might be more efficient.
4. Simultaneous fits (FIT2)
   - Free gap more flexible than assuming $\Delta_0 = 2M_\pi$.
   - Stat. errors smaller than summation method, GPOF; more stable than other methods.
   - No observable-dependent "tuning" of fit ranges, priors etc.
   - **Consistent fit for all observables and all ensembles (fixing $M_\pi t_{\mathrm{start}}$ globally).**

$\rightarrow$ **We choose simultaneous fits (FIT2) for our final analysis...**

Raw lattice results from simultaneous fit

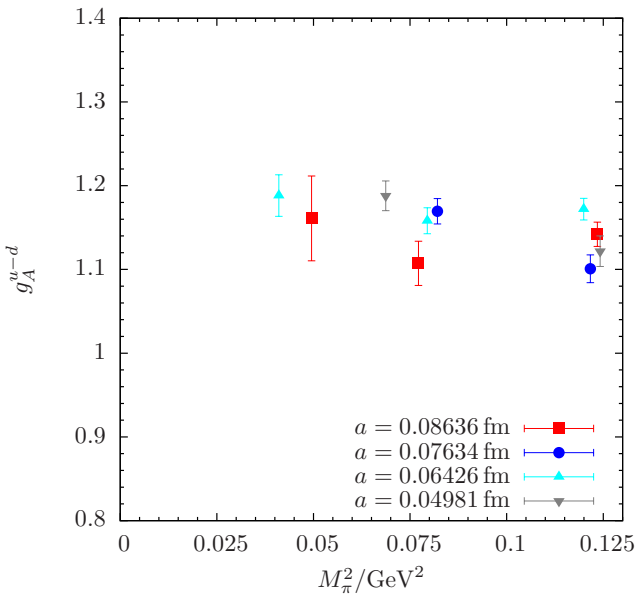

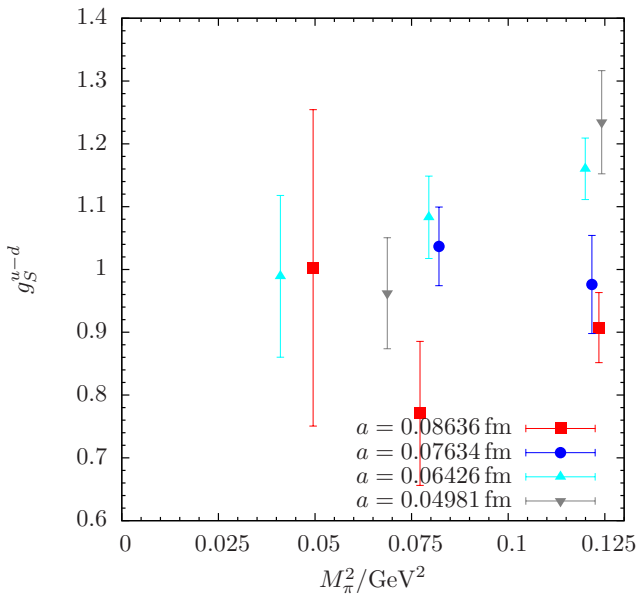

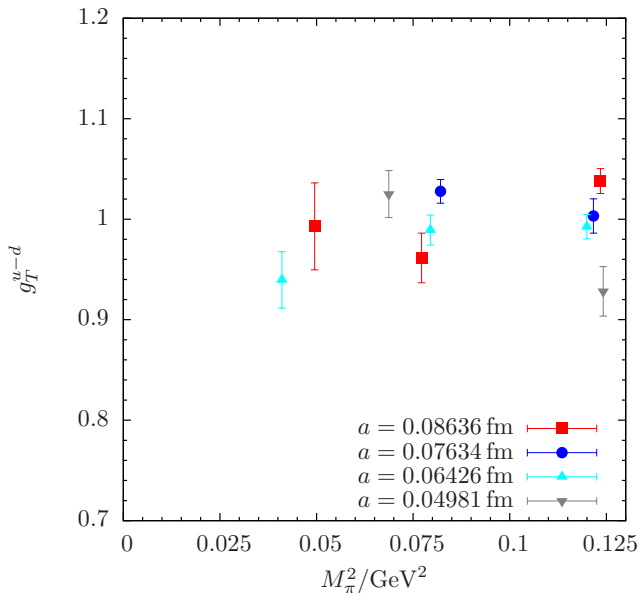

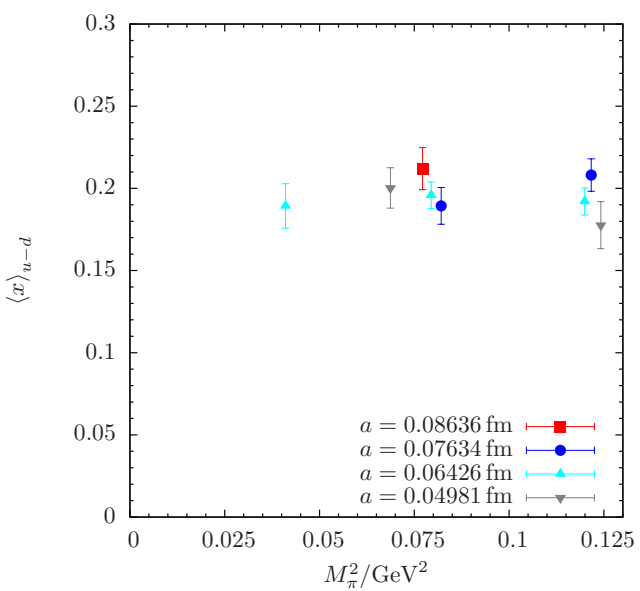

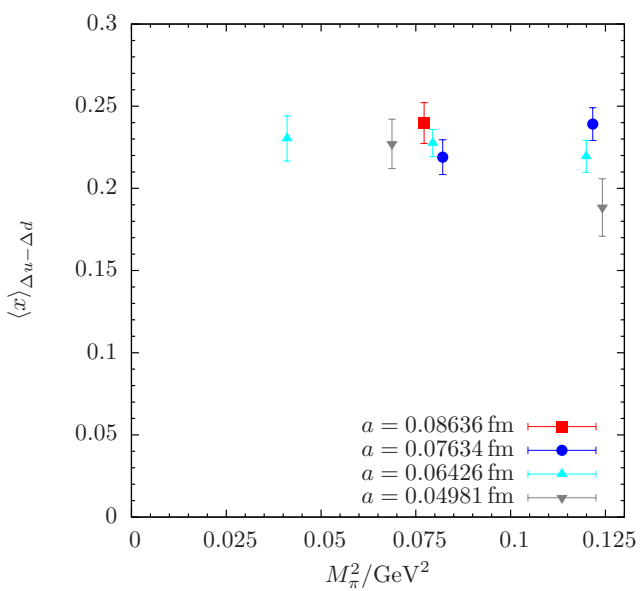

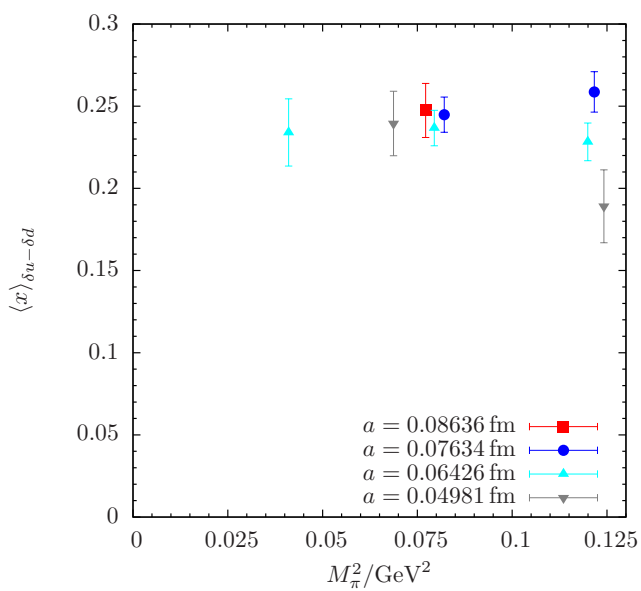

Chiral and continuum extrapolation

The (most general version) of our chiral and continuum fit model reads

$$O(M_\pi, a) = A_O + B_O M_\pi^2 + C_O M_\pi^2 \log M_\pi + D_O a^{n(O)}, \tag{18}$$

where

- $n(O) = \begin{cases} 2 & \text{if } O = g_A, g_S \\ 1 & \text{else} \end{cases}$,
- $A \equiv A_O$, $B \equiv B_O$, $C \equiv C_O$ and $D \equiv D_O$ are free fit parameters,
- For e.g. $O = g_A$ the coefficient C of the chiral log is known analytically, i.e.

$$C_{g_A} = \frac{-\mathring{g}_A}{(2\pi f_\pi)^2}\left(1 + 2\mathring{g}_A^2\right). \tag{19}$$

- We will denote specific fit models by the combination of letters used for the fit parameters of included term, e.g. "ABD".
- We find that in practice only fit models AB and ABD give reasonable results.
- Data not sensible to chiral logs, resulting in large values of χ^2/dof.
- We perform fits with and without a cut for data with $M_\pi > 290\,\mathrm{MeV}$.

Results for model ABD, no M_π-cut

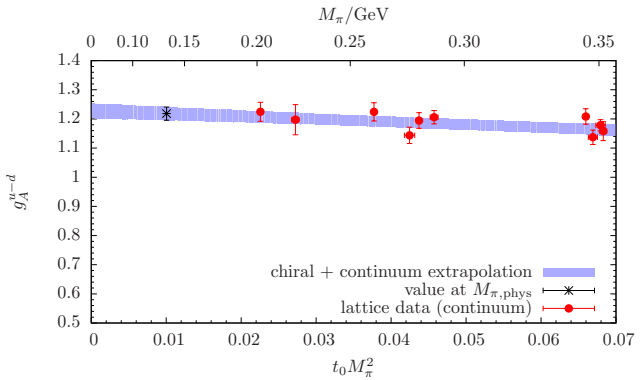

$\chi^2/dof = 2.37$

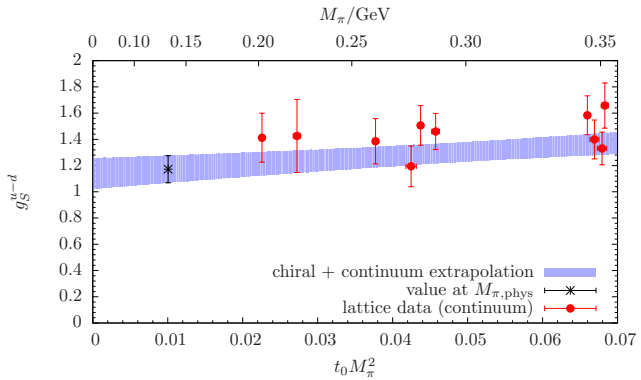

$\chi^2/dof = 1.09$

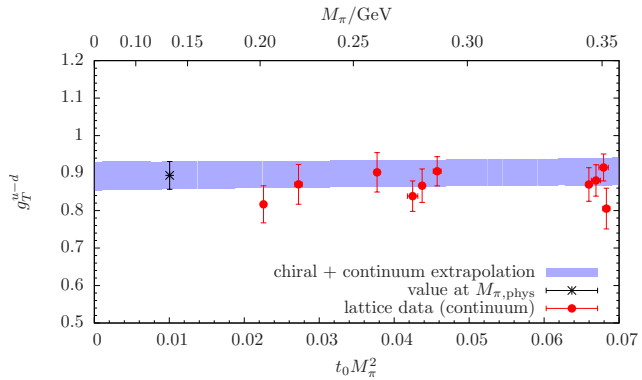

$\chi^2/dof = 3.19$

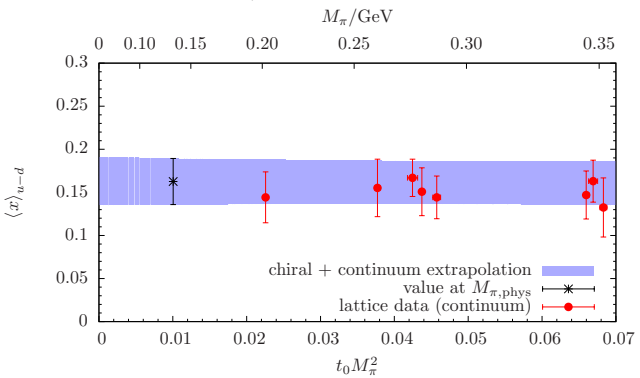

$\chi^2/dof = 0.72$

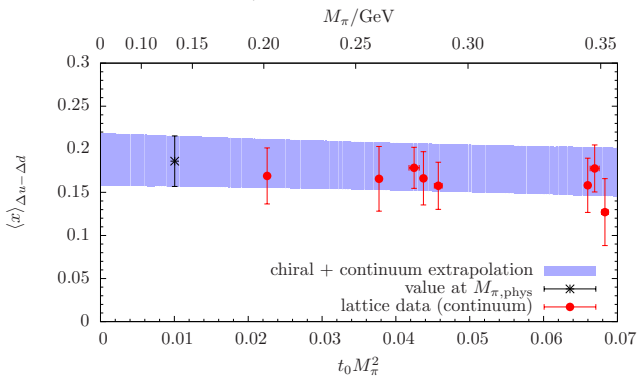

$\chi^2/dof = 0.99$

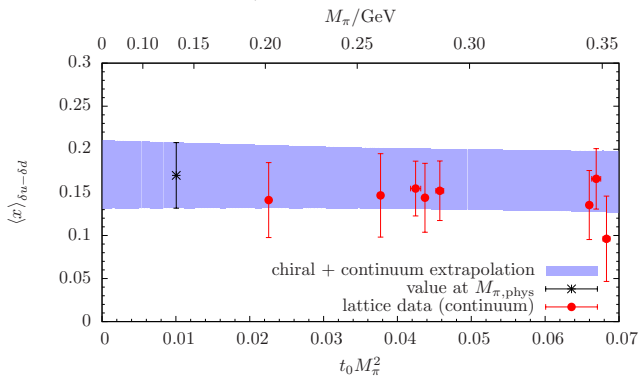

$\chi^2/dof = 0.88$

- Lattice data shown is corrected for continuum extrapolation.
- Results dominated by large ensembles with $M_\pi > 300\,\mathrm{MeV}$!
- Fit to g_T and g_A do not describe data very well...

Results for model ABD, $M_\pi < 290\,\mathrm{MeV}$

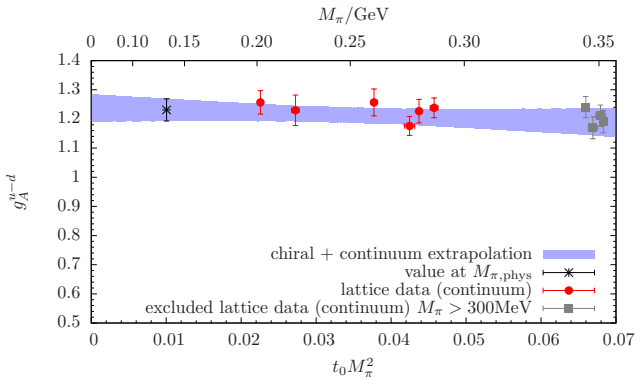

$\chi^2/dof = 1.12$

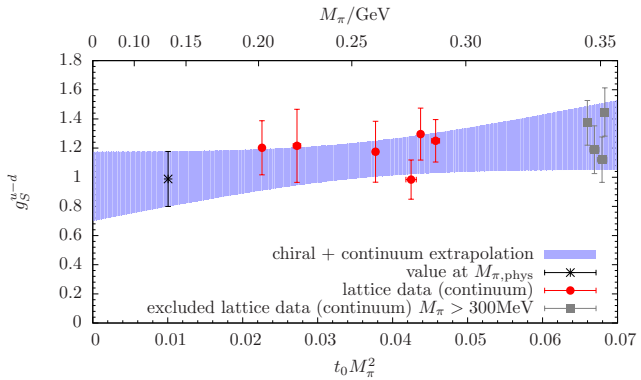

$\chi^2/dof = 1.53$

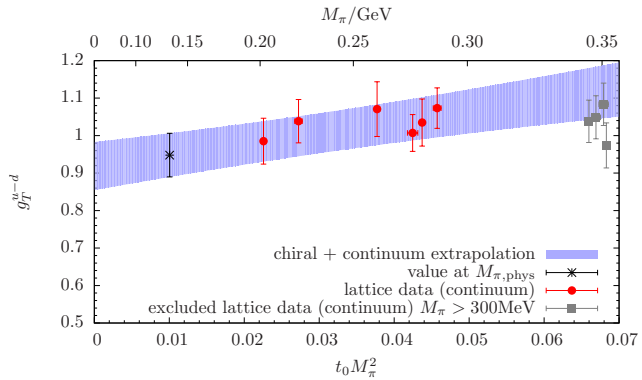

$\chi^2/dof = 2.75$

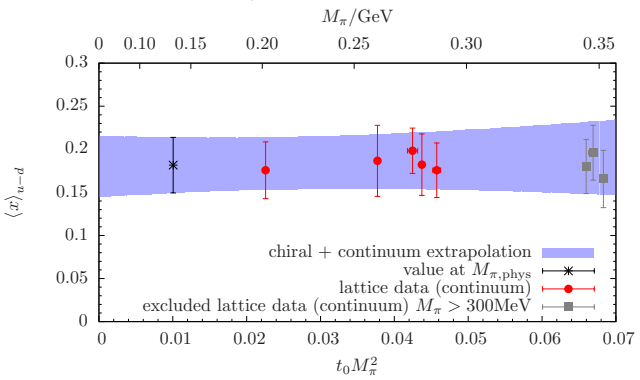

$\chi^2/dof = 1.02$

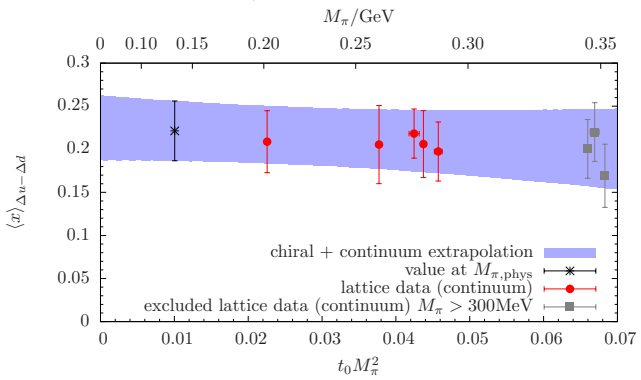

$\chi^2/dof = 0.65$

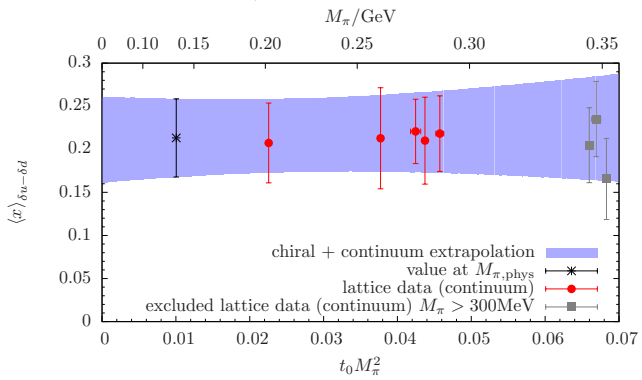

$\chi^2/dof = 0.85$

- Larger errors (as expected).
- Good χ^2/dof for g_A, also slightly improved for g_T.
- Chiral extrapolation very flat for twist-2 observables; but systematic shift observed.

Results for model AB, $M_\pi < 290\,\mathrm{MeV}$

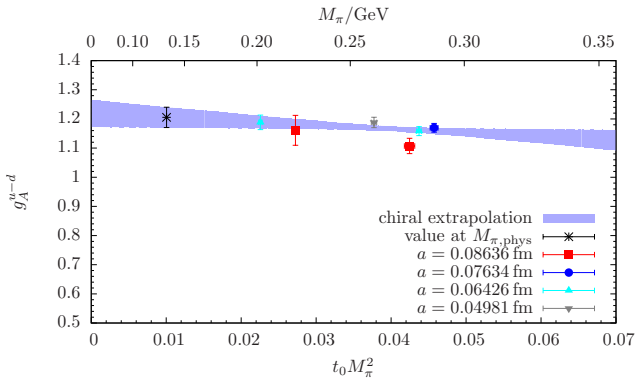

$\chi^2/dof = 1.55$

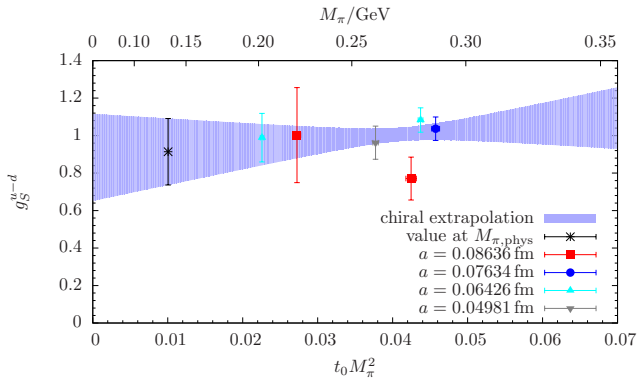

$\chi^2/dof = 1.47$

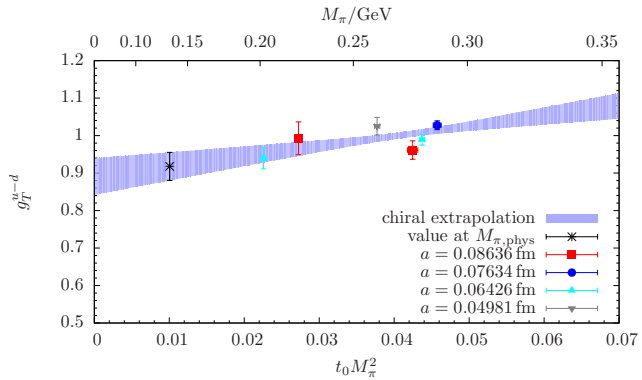

$\chi^2/dof = 2.18$

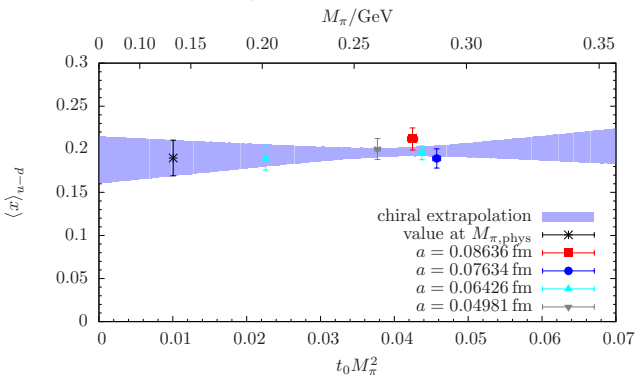

$\chi^2/dof = 0.72$

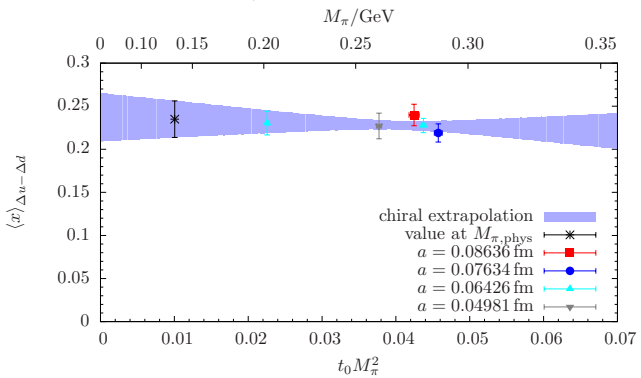

$\chi^2/dof = 0.52$

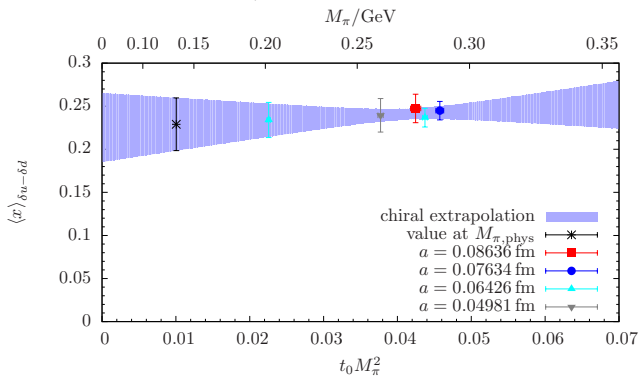

$\chi^2/dof = 0.13$

- Results without fitting term $\sim a$ / $\sim a^2$ compatible.
- Lattice artifacts are not well resolved but still sometimes $D_O \neq 0$ within errors!
- Fit model ABD should give more realistic errors.

Final results (still preliminary!)

Results for nucleon charges:

Fit		g_A^{u-d}	g_S^{u-d}	g_T^{u-d}
ABD,	$M_\pi < 290\,\mathrm{MeV}$	1.231(38)	0.99(19)	0.948(58)
ABD,	all M_π	1.218(23)	1.17(10)	0.894(37)
AB,	$M_\pi < 290\,\mathrm{MeV}$	1.205(35)	0.91(18)	0.918(37)
AB,	all M_π	1.199(18)	0.94(09)	0.988(18)

Results for lowest moments of dim-4 operators:

Fit		$\langle x \rangle_{u-d}$	$\langle x \rangle_{\Delta u - \Delta d}$	$\langle x \rangle_{\delta u - \delta d}$
ABD,	$M_\pi < 290\,\mathrm{MeV}$	0.182(32)	0.221(35)	0.213(45)
ABD,	all M_π	0.163(27)	0.186(29)	0.168(38)
AB,	$M_\pi < 290\,\mathrm{MeV}$	0.190(21)	0.235(21)	0.229(31)
AB,	all M_π	0.197(11)	0.234(12)	0.244(16)

- Scale setting uncertainty, error on renormalization etc. propagated into stat. errors.
- Residual excited state effects should also be reflected by this error.
- g_A still somewhat smaller than experimental value.
- Result for $\langle x \rangle_{u-d}$ in good agreement with phenomenological values.

Summary and Outlook

- We computed isovector charges and moments for local and twist-2 operators at four lattice spacings and for $M_\pi = 200 \ldots 350\,\mathrm{MeV}$.
- We investigated several methods to deal with excited states
- Simultaneous fits promising for controlling excited states at reasonable stat. error.
- **Consistent and observable-independent analysis / treatment of excited states.**
- Large t_{sep} (and small M_π) are important.
- Combined chiral and continuum extrapolation for all observables.

Ongoing work / future plans:

- Q^2-dependence, e.g. el.-mag. FF, axial FF, GFFs, $\mathcal{O}(a)$-improvement
- Inclusion of quark disconnected diagrams.
- Isoscalar observables, electro-strange FF ($\rightarrow$ quark disconnected diagrams)
- Include ensemble ($(T/a) \times (L/a)^3 = 192 \times 96^3$, $a = 0.064\,\mathrm{fm}$) at the physical point.

Backup slides

Chiral and continuum extrapolations – plateau method

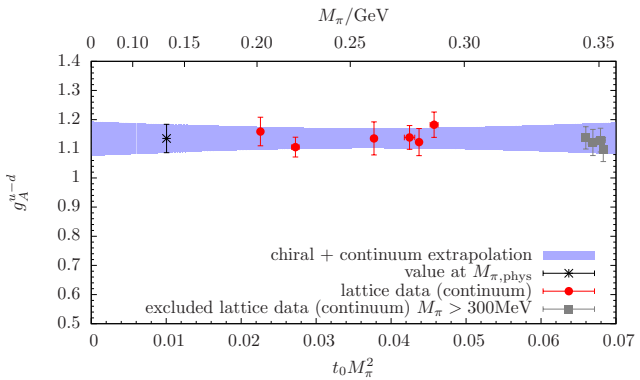

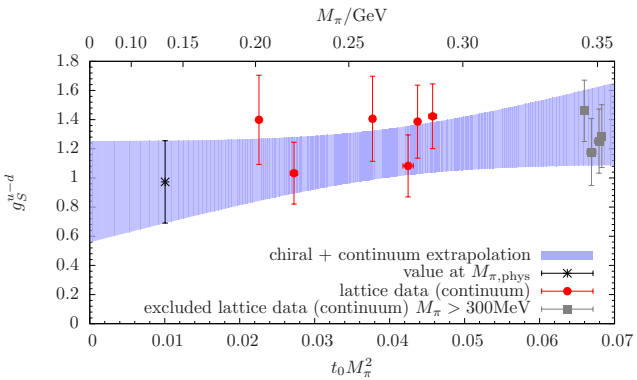

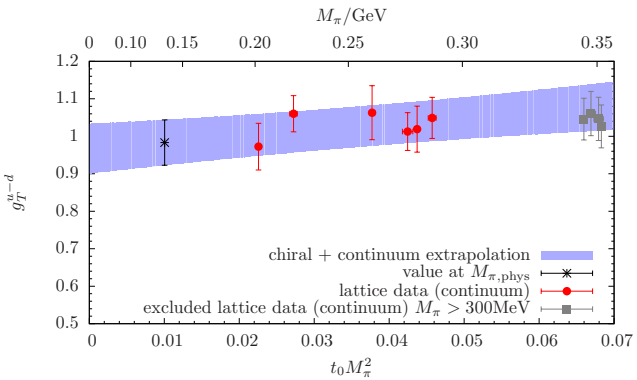

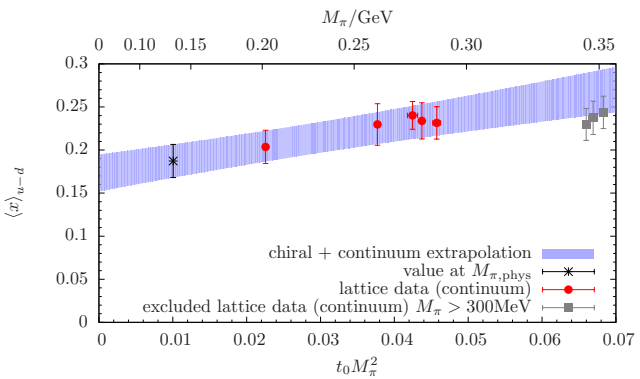

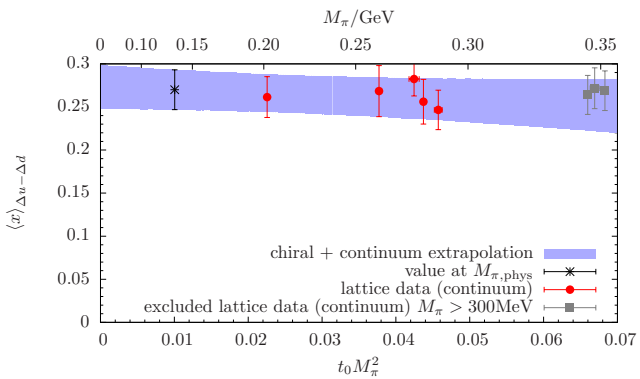

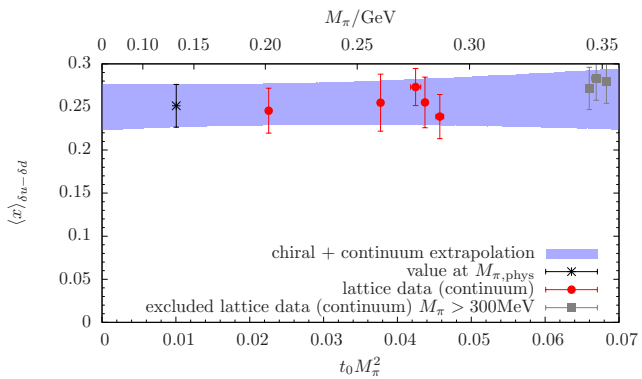

Chiral and continuum extrapolations – GPOF

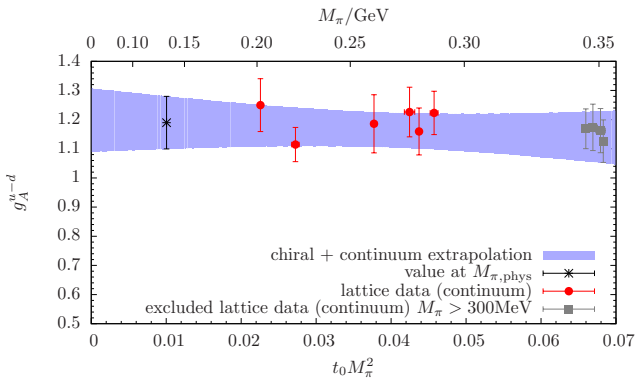

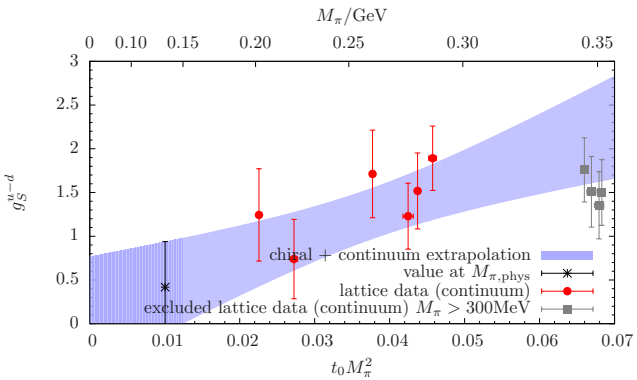

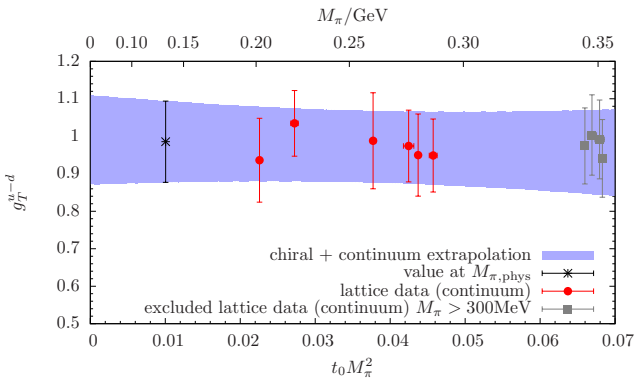

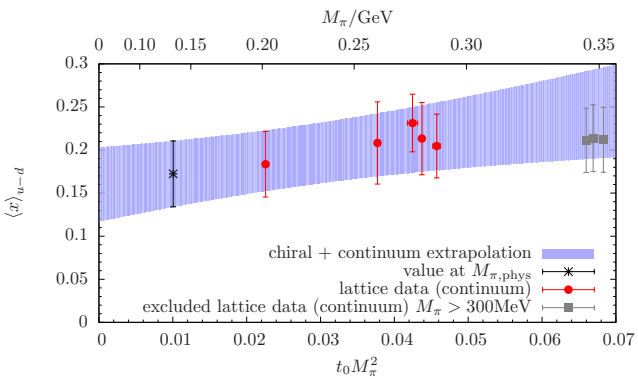

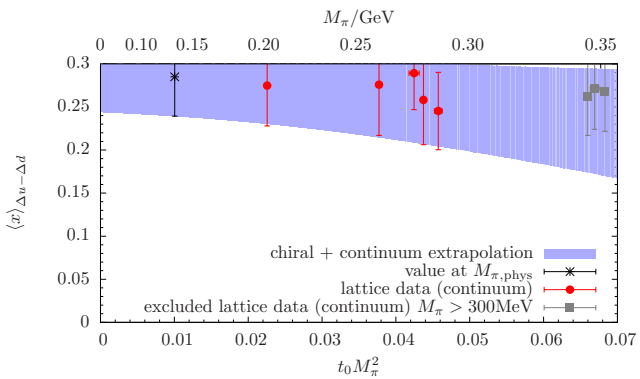

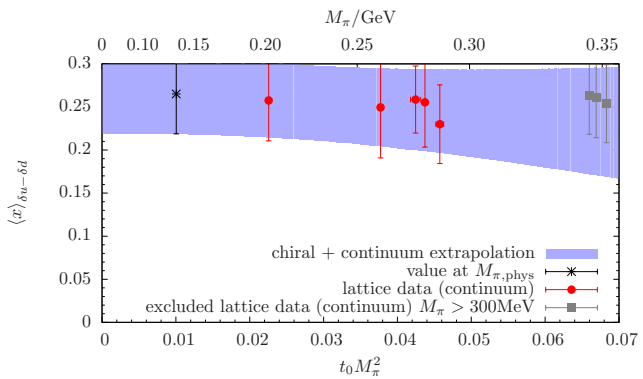

Chiral and continuum extrapolations – summation method

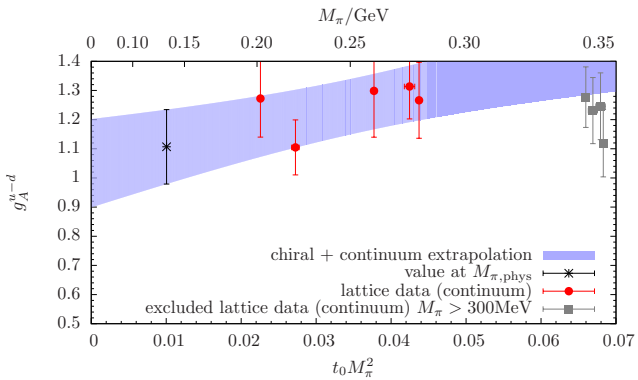

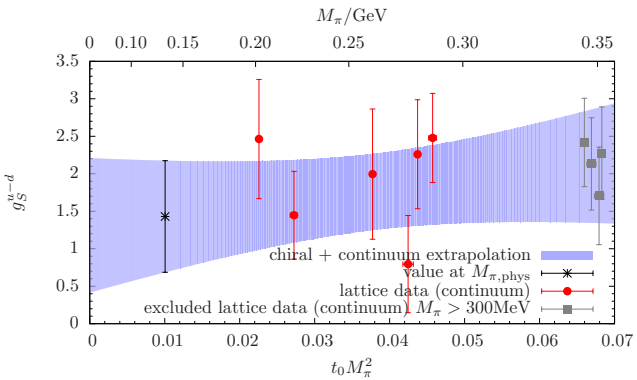

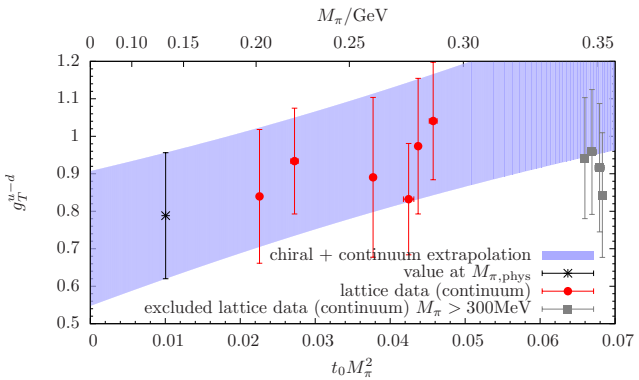

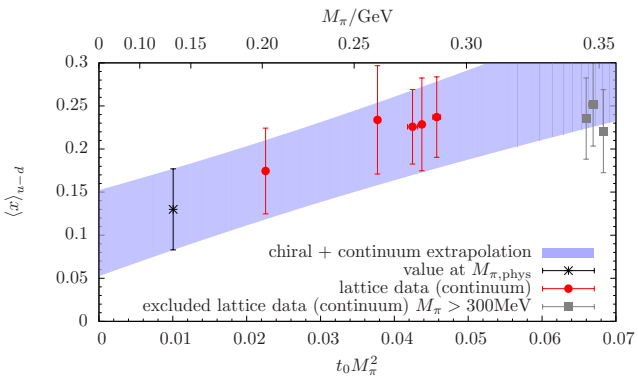

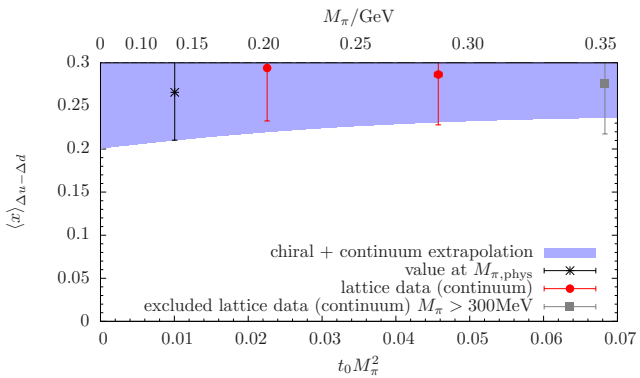

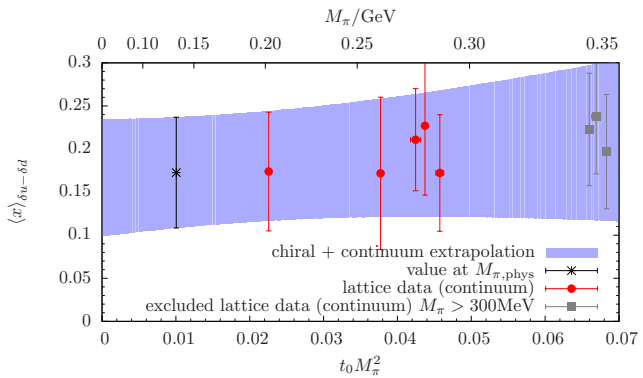

Chiral and continuum extrapolations – FIT2 $M_\pi t_{\text{start}} = 0.3$

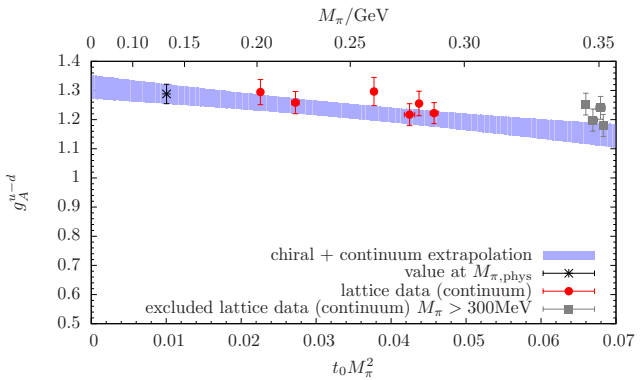

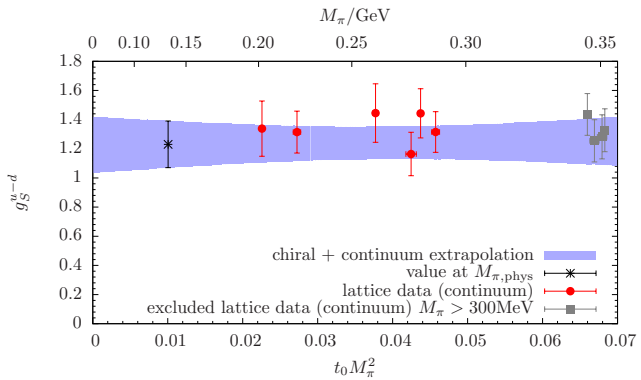

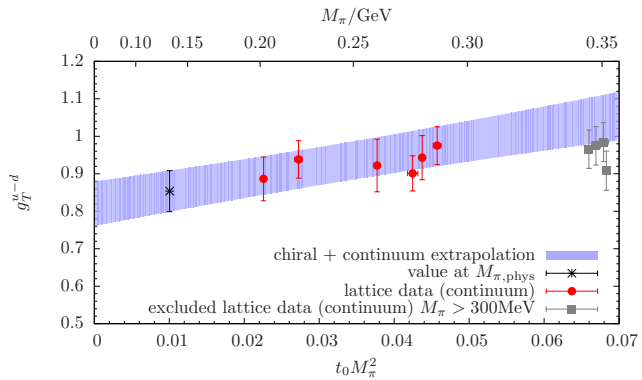

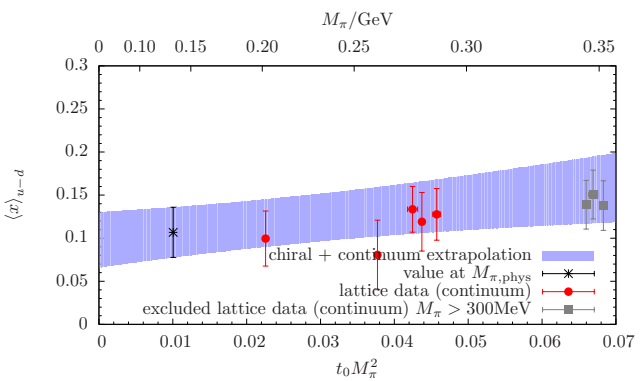

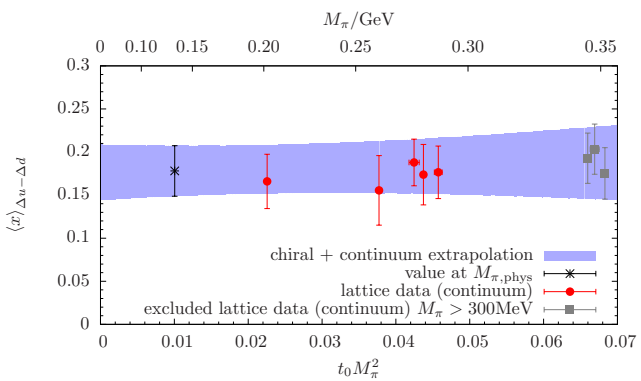

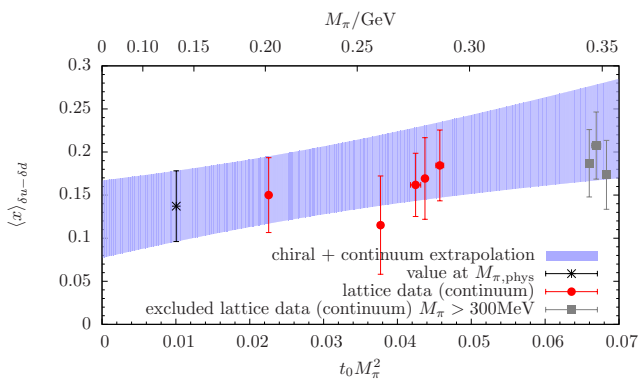

Chiral and continuum extrapolations – FIT2 $M_\pi t_{\text{start}} = 0.4$

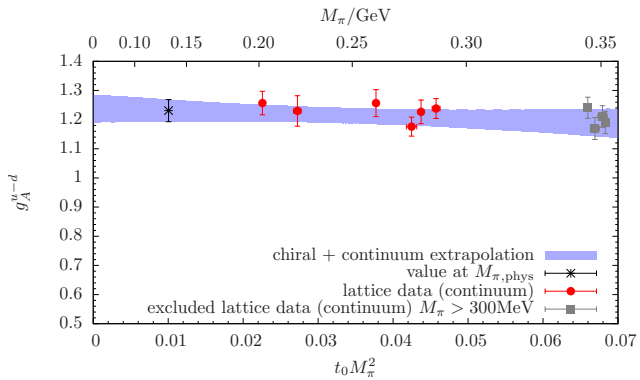

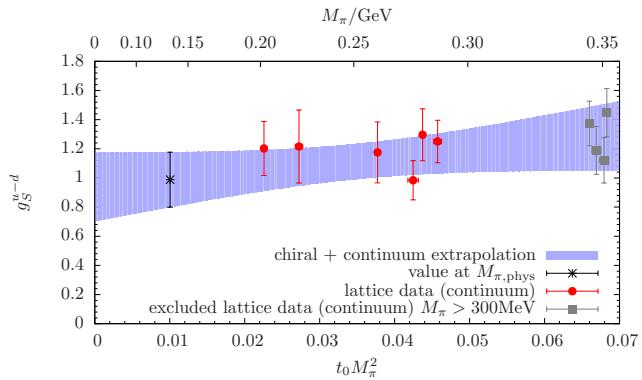

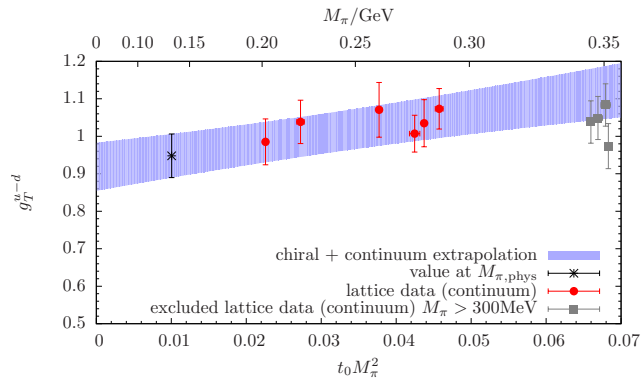

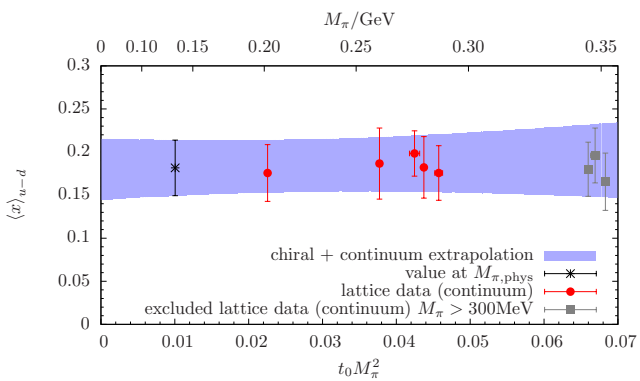

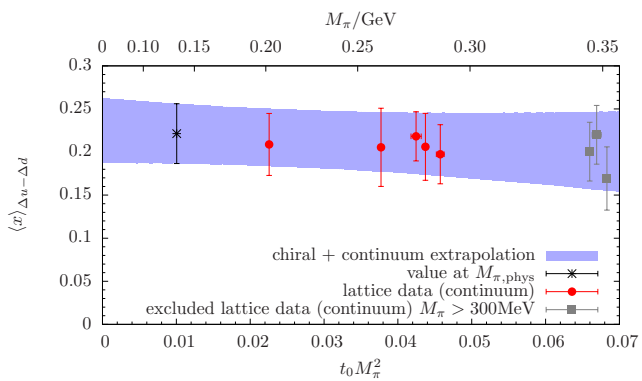

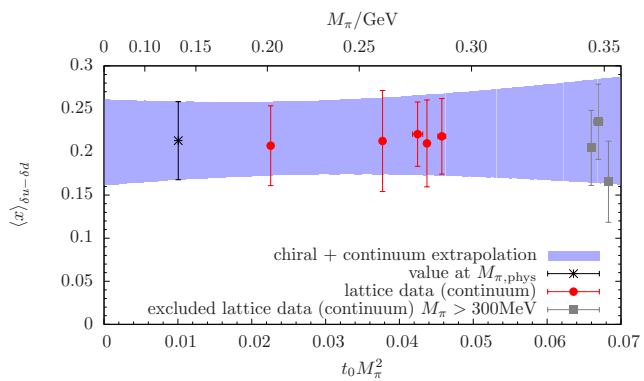

Chiral and continuum extrapolations – FIT2 $M_\pi t_{\text{start}} = 0.5$